Soft Computing (2022) 26:13899–13923
https://doi.org/10.1007/s00500-022-07417-w

APPLICATION OF SOFT COMPUTING

Application of Coulomb's and Franklin's laws algorithm to solve large-scale optimal reactive power dispatch problems

Mojtaba Ghasemi[1] · Ebrahim Akbari[2] · Iraj Faraji Davoudkhani[3] · Abolfazl Rahimnejad[4] · Mohammad Bagher Asadpoor[5] · Stephen Andrew Gadsden[4]

Accepted: 24 July 2022 / Published online: 19 September 2022

Abstract

This study focuses on the application of Coulomb's and Franklin's laws algorithm (CFA) to solving large-scale optimal reactive power dispatch (LS-ORPD) problems. The CFA optimizer acts on the basis of the charged particles interactions. The ever-increasing effects of ORPD problems for safe and reliable operation of electrical power grids is an important area of study. Such problems are classified as nonlinear optimization problems; the aim of which is to minimize the active power loss through tuning of several control variables. Firstly, the performance of CFA optimizer in solving high-dimensional problems is investigated using standard benchmark problems. Moreover, we apply the CFA optimizer for solving large-scale ORPD problems based on different constraints in three IEEE standard power systems. According to the results, the proposed optimizer offers a more accurate solution when compared with other methods found in the literature. Finally, an early attempt is carried out for improving CFA optimizer, which is tested on benchmark and ORPD problems and yields promising outcome in reaching a more powerful variant of CFA.

Keywords CFA optimizer · Optimization · Large-scale optimal reactive power dispatch (LS-ORPD) · Power grids

1 Introduction

Optimal reactive power dispatch (ORPD) problems have a substantial role with regard to the security requirements and energy management aspects of a power system. These problems specify the optimal working conditions of the system via providing the optimized power losses on the transmission lines along with meeting several pre-determined constraints. A number of control variables are utilized for this purpose, such as generator voltages, tap ratios of transformers, and reactive power of shunt VAr compensation devices. In its most general form, ORPD is a mixed integer, large-scale, non-linear multimodal, static optimization problem (Abido, 2006; Chen et al. 2017; de Souza et al. 2012; Deeb & Shahidehpour, 1990; Huang et al. 2012; Rojas et al. 2016).

During the last few decades, different evolutionary algorithms (EA) have been studied to address ORPD problems in various systems, including differential evolution (DE) algorithms (Ela et al. 2011; Liang et al. 2007; Shaheen et al. 2016; Varadarajan & Swarup, 2008), a hybridization of DE and evolutionary programming (EP) (Chung et al. 2010), DE with an efficient constraint handling (Mallipeddi et al. 2012), a modified DE (MDE) (Raha et al. 2012), a DE algorithm for ORPD problem while enhancing static voltage stability (Titare et al. 2014), a hybridization of chaotic artificial bee colony and differential evolution (CABC-DE) (Li et al. 2017). Swarm intelligence algorithms were also used for solving ORPD problems in many articles such as multi-agent-based PSO (MAPSO) (Zhao et al. 2005), a new improved PSO (ALC-

✉ Stephen Andrew Gadsden
gadsden@mcmaster.ca

1 Department of Electronics and Electrical Engineering, Shiraz University of Technology, Shiraz, Iran

2 Department of Electrical Engineering, Faculty of Engineering, University of Isfahan, Isfahan, Iran

3 Department of Electrical Engineering, Islamic Azad University, Khalkhal, Iran

4 Department of Mechanical Engineering, McMaster University, Hamilton, Canada

5 Department of Electrical and Computer Engineering, Semnan University, Semnan, Iran

PSO) (Singh et al. 2015), a new hybrid of PSO and imperialist competitive algorithms (PSO-ICA) (Mehdinejad et al. 2016), a hybrid topology scale-free Gaussian-dynamic PSO algorithm (Wang et al. 2014), the comprehensive learning PSO (CLPSO) (Mahadevan & Kannan, 2010), the ORPD within a wind farm using hybrid PSO (Kanna & Singh, 2015), a new PSO for ORPD using a novel fuzzy adaptive configuration (Naderi et al. 2017), an improved PSO for ORPD with static voltage stability (Hong-Zhong et al. 2010), PSO-based bio-inspired algorithms (Bhattacharyya & Raj, 2016), an improved pseudo-gradient search-PSO (IPG-PSO) to minimize real power loss, voltage stability index, and voltage deviation as the objective functions (Polprasert et al. 2016), seeker optimization algorithm (SOA) (Chaohua Dai et al. 2009; Shahbazi & Kalantar, 2013) using chaos scans in PSO (Tang et al. 2013), ant lion optimizer (ALO) (Mouassa et al. 2017), the enhanced Gaussian bare-bones water cycle algorithm (NGBWCA) (Heidari et al. 2017), the differential search algorithm (DSA) for ORPD with voltage control (Amrane et al. 2015), the biogeography-based optimization (BBO) (Roy et al. 2012a, b), accelerating bio-inspired optimizer (ABO) with transfer reinforcement learning (TRL) (Zhang et al. 2017), hybrid algorithms for ORPD with discrete control variables (M. Ghasemi et al. 2014a, b, c), an exchange market algorithm (EMA) (Rajan & Malakar, 2016), the gravitational search algorithm (GSA) (Duman et al. 2012; Roy et al. 2012a, b), a hybrid of PSO and GSA (Radosavljević et al. 2016), an opposition-based GSA (OGSA) (Shaw et al. 2014), an efficient hybrid algorithm using Nelder–Mead simplex search and shuffled frog leaping algorithm (Khorsandi et al. 2011), the harmony search algorithm (HSA) for ORPD and optimal voltage control (Khazali & Kalantar, 2011), the grey wolf optimizer (GWO) (Sulaiman et al. 2015), a hybrid Nelder-Mead simplex-based firefly algorithm (Rajan & Malakar, 2015), a fuzzy optimization model (Moghadam & Seifi, 2014), the chaos embedded krill herd algorithm (CEKHA) (Mukherjee & Mukherjee, 2016).

Moreover, optimal planning of different reactive power resources with AC-DC and FACTS controllers for OPF and ORPD problems was proposed in (Bhattacharyya & Kumar, 2015; Chowdhury et al. 2014; Thukaram & Yesuratnam, 2008). The multi-objective searching algorithms for solving multi-objective ORPD problem are also presented in the literature, some examples of which are a non-dominated sorting genetic algorithm-II (Azzam & Mousa, 2010; Jeyadevi et al. 2011; Ramesh et al. 2012; Zhihuan et al. 2010), a new modified GSA using opposition-based self-adaptive learning strategy (Niknam et al. 2013), multi-objective DE (Basu, 2016; Roselyn et al. 2014), a stochastic approach under load and wind power uncertainties (Mohseni-Bonab et al. 2016a, b), multi-objective ORPD considering voltage stability (Saraswat & Saini, 2013), a two-archive multi-objective grey wolf optimizer (TAMOGWA) (Nuaekaew et al. 2017), the adaptive multiple evolutionary algorithms (Hongxin et al. 2013), a multi-objective fuzzy-based procedure (Sehiemy et al. 2013), a new multi-objective strategy (A. Ghasemi et al. 2014a, b, c), a two-point estimate method for uncertainty modeling (Mohseni-Bonab et al. 2016a, b), strength Pareto multi-group search optimizer (SPMGSO) (Zhou et al. 2014) and, etc.

So far, various stochastic optimization algorithms have been employed to find solutions for miscellaneous optimization problems having practical complications, such as nonlinearity, non-convexity, mixed-integer nature, non-differentiability. These algorithms are modeled by principles and concepts extracted from the real-world nature, like collective birds and animal behaviors. For instance, some of these inspired algorithms are genetic algorithm (GA) (Mitchell, 1998), particle swarm optimization (PSO) (Eberhart & Kennedy, 1995), differential evolution (DE) (Storn & Price, 1997), imperialist competitive algorithm (ICA) (Atashpaz-Gargari & Lucas, 2007), artificial bee colony (ABC) (Karaboga & Basturk, 2007), intelligent water drops (IWD) algorithm (Hosseini, 2007), cuckoo search (CS) (Yang & Deb, 2009), gravitational search algorithm (GSA) (Rashedi et al. 2009), a novel competitive swarm optimizer (CSO) (Cheng & Jin, 2015), teaching–learning-based optimization (TLBO) algorithm and its modified versions (M. Ghasemi et al. 2015; M. Ghasemi et al. 2014a, b, c; Rao et al. 2011), mine blast algorithm (MBA) (Sadollah et al. 2013), and opposition-based algorithm (OBA) (Seif & Ahmadi, 2015), which have been proposed and applied for solving global numerical optimization problems (in the power systems as an example).

This paper proposes an application of the CFA optimizer, which is formed based on population and is inspired by the electrical interactions, for solving large-scale optimization problems including ORPD. The presented method yields a highly accurate solution when applied on various optimization problems. The efficiency of the proposed method in finding global solutions of large-scale optimization problems are examined with several benchmark test functions. A comparative study is made between CFA and other standard algorithms to discuss the basic aspects of CFA. Furthermore, a new version of CFA is proposed whose superiority over the original CFA was verified using benchmark functions and ORPD problems. Hence, the contributions of the paper are as follows:

- The application of CFA optimizer for solving ORPD problems and comparing its results with those of other recent methods in the literature.

- Proposing an improvement strategy to achieve a more efficient version of CFA optimizer and its verification using benchmark functions and ORPD problems.

The paper is organized as follows. The formulation of the ORPD problems is described in Sect. 2. The standard framework of the suggested algorithms is discussed and illustrated in Sect. 3. Section 4 summarizes the optimization results. Finally, conclusions and a brief summary of the study are provided in Sect. 5.

2 ORPD problem

ORPD problem as an efficient implementation in energy control and management of electrical power systems specifies the optimal working conditions of the system via providing an optimal value of P_{Loss} (real power loss) while meeting several constraints, with dependent variables x ($x^T = [V_{L1} \ldots V_{\text{LNPQ}}, Q_{G1} \ldots Q_{\text{GNG}}, S_{l1} \ldots S_{\text{lNTL}}]$) and control variables u ($u^T = [V_{G1} \ldots V_{\text{GNG}}, Q_{C1} \ldots Q_{\text{CNC}}, T_1 \ldots T_{\text{NT}}]$). Roughly speaking, ORPD makes an effort to minimize the active power loss via optimal tuning of control parameters subjected to a number of constraints (Basu, 2016; Ela et al. 2011).

The formulation of the ORPD problem is defined as follows (Ela et al. 2011; Wang et al. 2014):

$$\text{Min} J(x,u) = P_{\text{loss}} = \sum_{k \in NTL} g_k (V_i^2 + V_j^2 - 2V_iV_j\cos\delta_{ij}) \tag{1}$$

$$\text{Subject to}: g(x,u) = 0 \tag{2}$$

$$\text{and } h(x,u) \le 0 \tag{3}$$

where P_{loss} denotes the real power loss function of the transmission lines, g_k shows the conductance of branch k, V_i and V_j are the voltages of ith and jth bus, respectively, NTL gives the number of transmission lines, δ_{ij} is the voltage phase difference between bus i and bus j. Furthermore, x is the vector of dependent variables (state vector) and U is the vector of independent variables (decision variables), which are introduced in Table 1:

As a consequence, vector x is written as (4), and vector u is defined as in (5):

$$x^T = [V_{L1} \ldots V_{\text{LNPQ}}, Q_{G1} \ldots Q_{\text{GNG}}, S_{l1} \ldots S_{\text{lNTL}}] \tag{4}$$

$$u^T = [V_{G1} \ldots V_{\text{GNG}}, Q_{C1} \ldots Q_{\text{CNC}}, T_1 \ldots T_{\text{NT}}] \tag{5}$$

where NG shows the number of generators; NPQ denotes the number of PQ buses; NT is the number of tap-regulating transformers and NC is the number of shunt VAr compensators.

2.1 Constraints

2.1.1 Equality constraints

Based on the ORPD formulation, g in (2) represents the equality constraints, which are the power flow equations (Basu, 2016; Ela et al. 2011) as follows:

$$P_{Gi} - P_{Di} - V_i \sum_{j=1}^{\text{NB}} V_j [G_{ij}\cos(\delta_{ij}) + B_{ij}\sin(\delta_{ij})] = 0 \tag{6}$$

$$Q_{Gi} - Q_{Di} - V_i \sum_{j=1}^{\text{NB}} V_j [G_{ij}\sin(\delta_{ij}) - B_{ij}\cos(\delta_{ij})] = 0 \tag{7}$$

where NB denotes the number of buses in the system, P_{Gi} represents the amount of produced active power, Q_{Gi} is the amount of generated reactive power, P_{Di} and Q_{Di} denote the active and reactive load demands, respectively, and G_{ij} and B_{ij} express the conductance and susceptance values, respectively.

2.1.2 Inequality constraints

Based on the ORPD formulation, h in (3) represents the inequality constraints defined as follows:

i. Generator constraints: the active power generation of the slack bus, voltage magnitudes and reactive power outputs of the generation buses are constrained by the associated lower and upper boundaries:

$$\begin{aligned} P_{G,\text{slack}}^{\min} \le P_{G,\text{slack}} \le P_{G,\text{slack}}^{\max} \\ V_{Gi}^{\min} \le V_{Gi} \le V_{Gi}^{\max}, \quad i = 1, \ldots, \text{NG} \\ Q_{Gi}^{\min} \le Q_{Gi} \le Q_{Gi}^{\max}, \quad i = 1, \ldots, \text{NG} \end{aligned} \tag{8}$$

where $V_{Gi}^{\min}$ and $V_{Gi}^{\max}$ denotes the minimum and maximum voltages of the ith generation unit; $P_{Gi}^{\min}$ and $P_{Gi}^{\max}$ represent the minimum and maximum active power outputs of the ith generation unit; and $Q_{Gi}^{\min}$ and $Q_{Gi}^{\max}$ denote the minimum and maximum reactive power outputs of the ith generation unit, respectively.

ii. Limitations on transformers: tap settings of transformers are constrained via the corresponding lower and upper boundaries as follows:

$$T_i^{\min} \le T_i \le T_i^{\max}, \quad i = 1, \ldots, \text{NT} \tag{9}$$

where $T_i^{\min}$ and $T_i^{\max}$ are the minimum and maximum boundaries, respectively, for tap settings of the ith transformer.

Table 1 State and decision variables of ORPD problem

State variables		Decision variables	
V_L	Voltage of load buses	V_G	Voltages of generator buses, (continuous decision variable)
Q_G	Output reactive power of generators	T	Settings of transformer taps, (discrete decision variable)
S_l	Loading (or line flow) of transmission lines	Q_C	Shunt VAr compensation (discrete decision variable)

iii. Limitations on shunt VAr compensators: Shunt VAr compensations are constrained based on the following equation:

$$Q_{Ci}^{\min} \le Q_{Ci} \le Q_{Ci}^{\max}, \quad i = 1, \ldots, \mathrm{NC} \tag{10}$$

where $Q_{Ci}^{\min}$ and $Q_{Ci}^{\max}$ represent the lower and upper boundaries, respectively, for VAr injection of the ith shunt compensator.

iv. Security constraints: These constraints are associated with the voltage limits of the load buses and the loading limit (capacity) of the transmission lines:

$$V_{Li}^{\min} \le V_{Li} \le V_{Li}^{\max}, \quad i = 1, \ldots, \mathrm{NPQ} \tag{11}$$

$$S_{li} \le S_{li}^{\max}, \quad i = 1, \ldots, \mathrm{NTL} \tag{12}$$

where $V_{Li}^{\min}$ and $V_{Li}^{\max}$ represent the lower and upper voltage limits of the ith load bus, respectively. Furthermore, S_{li} is the apparent power flow on the ith branch and $S_{li}^{\max}$ represents the upper limit of the apparent power flow on the ith branch.

It should be noted that in order to include the inequality constraints into the objective function, the penalty terms are defined and Eq. (1) may be rewritten accordingly (Shahbazi & Kalantar, 2013):

$$F_{\mathrm{ORPD}} = P_{\mathrm{Loss}} + \lambda_V \sum_{i \in N_V^{\lim}} (V_i - V_i^{\lim})^2 + \lambda_Q \sum_{i \in N_Q^{\lim}} (Q_{Gi} - Q_{Gi}^{\lim})^2 + \lambda_S \sum_{i \in N_S^{\lim}} (S_{li} - S_{li}^{\lim})^2 \tag{13}$$

where λ_V,λ_Q and λ_S are the penalty coefficients, $N_V^{\lim}$,$N_Q^{\lim}$ and $N_S^{\lim}$ express the number of buses where voltage violates and exceeds the specified limits, the number of generator buses on which the injected reactive power violates the specified limits, and the number of the transmission lines on which the loading violates the defined limits. Furthermore, $V_i^{\lim}$, $Q_{Gi}^{\lim}$, and $S_{li}^{\lim}$ are defined as follows:

$$V_i^{\lim} = \begin{cases} V_i, & \text{if } V_i^{\min} \le V_i \le V_i^{\max} \\ V_i^{\min}, & \text{if } V_i < V_i^{\min} \\ V_i^{max}, & \text{if } V_i > V_i^{\max} \end{cases} \tag{14}$$

$$Q_{Gi}^{\lim} = \begin{cases} Q_{Gi}, & \text{if } Q_{Gi}^{\min} \le Q_{Gi} \le Q_{Gi}^{\max} \\ Q_{Gi}^{\min}, & \text{if } Q_{Gi} < Q_{Gi}^{\min} \\ Q_{Gi}^{\max}, & \text{if } Q_{Gi} > Q_{Gi}^{\max} \end{cases} \tag{15}$$

$$S_{li}^{\lim} = \begin{cases} S_{li}, & \text{if } S_{li} \le S_{li}^{\max} \\ S_{li}^{\max}, & \text{if } S_{li} > S_{li}^{\max} \end{cases} \tag{16}$$

3 CFA optimizer

CFA is a powerful and efficient optimization algorithm proposed by Ghasemi et al. in 2018 (M. Ghasemi et al. 2018), which is inspired by governing rules of nature on charges and objects that constitute things and materials. This algorithm is very robust and strong to deal with optimization problems, especially high-dimensional classic ones. In CFA, it is assumed that there are a certain number of charged objects and each object is comprised of a definite number of electrical charges, where each individual electrical charge itself consists of a number of base charges equal to the dimension of the optimization problem. Objects, as depicted in Fig. 1, interact based on physics laws according to their sign, whether positive or negative (here they are modeled in the form of their objective functions), and accordingly attract (the distance between them decreases) or repel (the distance between them increases) each other. A solution or individual with a better objective value than the considered solution or member (x_j) is assumed as the attractor determined by an opposite sign with respect to the considered solution $\left(\mathrm{mean}\left(\sum_{m=1 \in \mathrm{Ob}_i}^{a, a \le a_{\max}} x_i^{\mathrm{Better-than-x}_j}\right)\right)$ and cause the considered solution to move toward it. On the other hand, a solution with a worse objective value is assumed as the repeller, determined by the same sign as the considered solution $\left(\mathrm{mean}\left(\sum_{m=1 \in \mathrm{Ob}_i}^{r, r \le r_{\max}} x_m^{\mathrm{Worse-than-x}_j}\right)\right)$ and forces the considered solution or member to move away from it. Each object

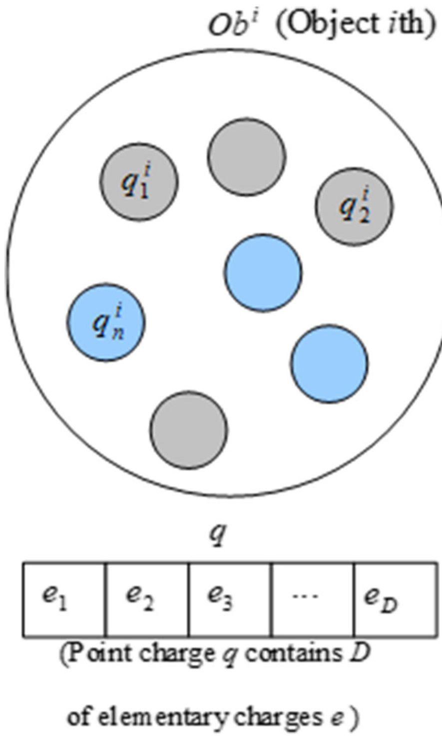

Fig. 1 Illustration of the i-th object containing positive and negative charges

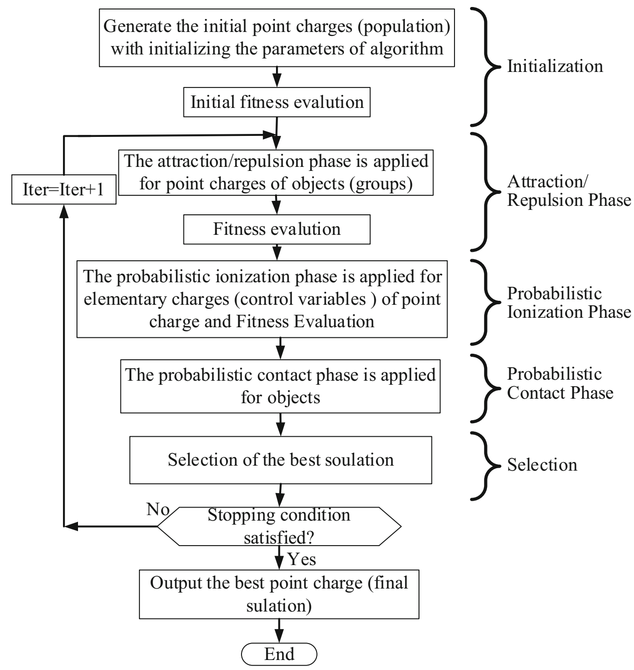

Fig. 2 Steps of the CFA optimizer

or solution always tends to move away from the solution with the worst fitness value (x^{Worst}) and approach the solution with the best fitness value (x^{Best}), and this is the basis of the optimization approach in this algorithm.

Furthermore, the charged objects will have the same electrical charge after they are contacted to each other. Hence, the algorithm population is divided into several groups/objects, where the transfer of any individual from one group to another is equivalent to the electrical charge transfer between two objects.

Mathematical descriptions of Coulomb's and Franklin's laws (M. Ghasemi et al. 2018) are exploited here to explain the procedure of the CFA optimizer. Figure 2 depicts the steps of the optimizer, which are explained in the following sub-sections.

3.1 Initial population

First, an initial population is formed by creating N electrical charges. The charges are established as D-dimension vectors. All elements of the vectors are constrained within the limits of the corresponding decision variable. For instance, the limits for the k-th element are denoted as $\left[x_k^{\min}, x_k^{\max}\right]$. Employing a uniform random variable generated in the interval of [0, 1], i.e. U[0, 1], we can obtain the q_j^i quantity over the feasible solution space:

$$q_{j,k}^i = x_k^{\min} + \mathrm{U}[0,1] * \left(x_k^{\max} - x_k^{\min}\right), \text{ for } k = 1, \cdots, D \tag{17}$$

3.2 Selecting the favorite objects for the number of objects greater than one

In case *Nob* (the number of objects) is equal to one, the whole population are allocated to a single group. When there is more than one object, i.e., *Nob* is equal to or greater than 2, the initial population is firstly arranged based on their corresponding objective function values, ordered from the best to the worst member. After that, these sorted members are allocated to *Nob* distinct groups, where different groups represent different corresponding objects. The population grouping is performed as such the first *Nob* best members (chosen from the sorted members) are allocated to the *Nob* groups one by one, and then the second *Nob* members are again dedicated to the *Nob* groups one by one, and so on. This procedure is iterated until all members are allocated to the corresponding groups.

3.3 The attraction/repulsion stage

In the attraction/repulsion stage, the objective function values corresponding to the i-th group's members are used to sort the members. To find the new position of the j-th member (x_j^{new}) belonging to the i-th group (Ob_i) using an attraction/repulsion-based mathematical description, explained in the Subsection 3.1, *a/r* members of the i-th object are selected in a random way. The costs of these members for attraction/repulsion stage are less/more than that of x_j. Next, the average values of attraction and repulsion vectors are obtained which are equal to $\text{mean}\left(\sum_{m=1\in \text{Ob}_i}^{a,a\le a_{\max}} x_i^{\text{Better-than-x}_j}\right)$ and $\text{mean}\left(\sum_{m=1\in \text{Ob}_i}^{r,r\le r_{\max}} x_m^{\text{Worse-than-x}_j}\right)$, respectively. Eventually, constant) is greater than $rand$ (contact probability factor) in any iteration, then the contact operation will be executed for that iteration. After testing different values, $Pc = 0.5$ was found as the value that gives the best solutions for all the performed simulations. Equation (20) expresses the formulation of this stage:

$$\begin{cases} x^{\text{Best}_1} = x^{\text{Best}_{Nob}},\ \ldots, x^{\text{Best}_{i+1}} = x^{\text{Best}_i},\ \ldots,\ x^{\text{Best}_{Nob}} = x^{\text{Best}_{Nob-1}} \\ x^{\text{Worst}_1} = x^{\text{Worst}_{Nob}},\ \ldots, x^{\text{Worst}_{i+1}} = x^{\text{Worst}_i},\ \ldots,\ x^{\text{Worst}_{Nob}} = x^{\text{Worst}_{Nob-1}} \end{cases} \text{if } \text{rand}_{\text{Iter}} \le Pc \text{ and } Nob \ge 2 \tag{20}$$

x_j^{new} is found based on (18). Provided that the objective function of x_j^{new} is more suitable (less for minimization) than that of x_j, $\left(f\left(x_j^{\text{new}}\right) \le f\left(x_j^{\text{old}}\right)\right)$, then the new position of x_j is acceptable; otherwise, the previous position of x_j., i.e. x_j^{old}, is preserved.

$$\begin{aligned} x_j^{\text{new}} &= x_j^{\text{old}} + \left|\cos\theta_j^{\text{new}}\right|^2 \times \left(x^{\text{Best}} - x^{\text{Worst}}\right) \\ &+ \left|\sin\theta_j^{\text{new}}\right|^2 \times \left(\text{mean}\left(\sum_{m=1\in \text{Ob}_i}^{a,a\le a_{\max}} x_m^{\text{Better-than-x}_j}\right)\right. \\ &\left. -\text{mean}\left(\sum_{m=1\in \text{Ob}_i}^{r,r\le r_{\max}} x_m^{\text{Worse-than-x}_j}\right)\right) \end{aligned} \tag{18}$$

3.4 Probabilistic ionization stage

Probabilistic ionization stage is accomplished separately for individual members. The ionization occurs merely for the k-th decision variable of x_j ($x_{j,k}$). In case the amount of normalized ionization energy, Pi, for the j-th member (x_j) surpasses a randomly selected value, $rand$, $x_{j,k}$ will be chosen in a random way by utilizing $k = \text{round}(1 + \text{rand} * (D - 1))$, where D denotes the dimension of the problem. Two parameters are used to attain the new control variable $x_{j,k}^{\text{new}}$, namely the k-th decision variable and the best and worst members of an identical group, x^{Best} and x^{Worst}:

$$x_{j,k}^{\text{new}} = x_k^{\text{Best}} + x_k^{\text{Worst}} - x_{j,k}^{\text{old}} \tag{19}$$

3.5 The probabilistic contact stage for a multi-object CFA optimizer

For multi-object (or equally multi-group) optimizer, when Nob is equal or greater than 2, specifically when dealing with high-dimensional problems, provided that Pc (the

4 A comparative study of CFA optimizer

To demonstrate the high performance and superiority of the presented method, in this section the performance of CFA optimizer compared to that of the classical algorithms proposed in the preceding research studies for six conventional standard test functions (benchmarks) listed in Table 2. The chosen classical methods in this study include the PSO (http://www.mathworks.com/matlabcentral/) (Eberhart & Kennedy, 1995), DE (model DE/best/1) (http://academic.csuohio.edu/simond/bbo/) (Storn & Price, 1997), ABC (http://mf.erciyes.edu.tr/abc/) (Karaboga & Basturk, 2007), and CS (http://www.mathworks.com/matlabcentral/) (Yang & Deb, 2009). It should be noted that the parameters considered for these algorithms are derived from the relevant references.

In the first sub-section, the single-object CFA optimizer is used to attain the optimal solution for the above-mentioned benchmark functions with a population size equal to 5. Then, multi-object CFA optimizer model will be used to solve the ORPD problem as a real-world case study.

4.1 Single-object CFA optimizer for traditional test functions

In this sub-section, six high-dimensional unimodal and multimodal benchmarks (with different number of dimensions) are chosen to assess the efficiency and capabilities of the suggested algorithm (CFA optimizer) compared to other methods such as PSO, DE/best/1, ABC, and CS. In this section, the presented single-object CFA optimizer model with five-point charges is used (with $Nob = 1$ and $N = 5$).

All algorithms were executed 30 times for each test function (listed in Table 2) with different number of dimensions and the means (Mean) and standard deviations (Std.) of the optimal solutions are presented in Table 3. The simulation results show that CFA optimizer is a powerful

Table 2 The traditional test functions

Name	Test function	Search Range	Global optimum
Sphere	$f_1(x) = \sum_{j=1}^{D} x_j^2$	$[-100, 100]^D$	0.0
Rastrigin	$f_2(x) = \sum_{j=1}^{D} \left(x_j^2 - 10\cos(2\pi x_j) + 10\right)$	$[-5.12, 5.12]^D$	0.0
Rosenbrock	$f_3(x) = \sum_{j=1}^{D-1} \left(100\left(x_j^2 - x_{j+1}\right)^2 + (x_j - 1)^2\right)$	$[-30, 30]^D$	0.0
Schwefel's	$f_4(x) = \sum_{j=1}^{D} \left(-x_j \sin\left(\sqrt{\lvert x_j \rvert}\right)\right)$	$[-500, 500]^D$	$-418.9829*D$
Griewank	$f_4(x) = \frac{1}{4000}\sum_{j=1}^{D-1} x_j^2 - \prod_{j=1}^{D}\cos\left(\frac{x_j}{\sqrt{j}}\right) + 1$	$[-600, 600]^D$	0.0
Weierstrass	$f_7(x) = \sum_{j=1}^{D}\left(\sum_{k=0}^{k\ \max}\left[a^k\cos\left(2\pi b^k(x_j + 0.5)\right)\right]\right) - D\sum_{k=0}^{k\ \max}\left[a^k\cos(\pi b^k)\right],\ a = 0.5,\ b = 3,\ k\ \max = 20.$	$[-0.50, 0.50]^D$	0.0

tool to obtain the optimal solution for high-dimensional problems (like $D = 25{,}000$) with very small population size ($N = 5$), and provides a significantly better solution compared to PSO, DE/best/1, ABC and CS algorithms. Convergence performance of all algorithms are shown in Figs. 3a–d and 4a–d for f_1 and f_5 with four different number of dimensions. The results show that CFA optimizer is capable of obtaining the global optimal solution in small number of iterations even for $D = 25{,}000$ and $N = 5$; this shows the fast convergence capability of CFA optimizer.

Overall, according to the experimental results presented in Table 3 and Figs. 3 and 4, we may list the following features for CFA optimizer:

1. CFA optimizer is able to provide global optimal solution for the higher-dimensional test functions with a small constant population $N = 5$ even for $D = 25{,}000$.
2. The population size and iterations (convergence rate) of CFA optimizer to achieve the global optimal solution is almost independent from problems' dimension for different test functions, and CFA algorithm is stable and robust as well.
3. CFA optimizer has fast convergence rate and, consequently, low computational cost even for high-dimensional test functions.
4. CFA optimizer requires constant control parameters for all test functions, i.e., $Pi = 0.01$ and $Pc = 0.5$.

4.2 Multi-object CFA optimizer

In this sub-section, the multi-object CFA optimizer is used to obtain optimal solution for shifted benchmark functions.

4.2.1 Why multi-object CFA optimizer and shifted benchmark functions?

In the second phase of the simulation, we evaluate the performance of CFA optimizer for different number of objects. In this regard, one may ask: what is the reason behind assessing the effect of the number of objects? Based on the results given in Table 3, when the population size is increased the optimization power of CFA optimizer decreases to some extent (see Fig. 5). Hence, it can be concluded that the probability of trapping in the local optima is greater than the case with smaller population; this challenge may be encountered in the large-scale practical optimization problems. Considering the same conditions presented in the first phase of simulations, the optimal results achieved after 30 runs are reported in Table 4, based on which it can be deduced that the optimization power of CFA increases by increasing the number of objects. In this case, the algorithm avoids form being trapped in the local optima specifically when $N/N_{ob} = 5$. Note that this value is not necessarily the best population size for each object/group for any given functions. The convergence rate of the multi-object CFA optimizer with respect to the number of objects for the shifted Sphere function with $D = 600$ is depicted in Fig. 6.

5 Multi-object CFA optimizer for large-scale ORPD

To demonstrate the efficiency and superiority of the proposed method, the CFA optimizer along with other algorithms are applied to obtain the optimal solution for the

Table 3 Results obtained by optimization algorithms for test functions with time

Algorithms	D = 200		D = 1000		D = 5000		D = 25,000	
	Mean	Std	Mean	Std	Mean	Std	Mean	Std
f_1: Sphere function								
PSO	489.0570	80.6111	1.3176e + 004	1.4774e + 003	9.7531e + 004	1.1804e + 004	4.2919e + 005	1.0141e + 005
DE/best/1	0.1768	0.2366	3.8957e + 005	3.2786e + 004	6.4798e + 006	3.4831e + 005	6.885e + 007	6.0072e + 006
ABC	9.5348e-06	8.0189e-06	2.1032e + 005	2.2642e + 004	1.0092e + 007	1.1957e + 005	7.5657e + 007	3.7624e + 005
CS	83.0543	4.9207	2.0026e + 004	1.6628e + 003	4.6891e + 005	2.7071e + 004	3.9720e + 006	6.1504e + 004
CFA	0.0	0.0	0.0	0.0	0.0	0.0	2.19e-329	0.0
f_2: Rastrigin's function								
PSO	336.1310	43.9162	5.5583e + 003	169.5787	3.8357e + 004	1.3272e + 003	1.3615e + 005	9.4763e + 003
DE/best/1	794.2286	119.3455	7.6192e + 003	121.0999	5.8558e + 004	478.6978	3.6054e + 005	3.4489e + 003
ABC	55.0851	3.9590	4.1075e + 003	116.5710	6.2322e + 004	369.6089	4.2492e + 005	2.6639e + 003
CS	998.053	57.0146	8.0760e + 003	143.1086	4.9448e + 004	281.3829	2.805e + 005	682.2473
CFA	0.0	0.0	0.0	0.0	0.0	0.0	0.0	0.0
f_3: Rosenbrock's function								
PSO	1.4165e + 004	3.7093e + 003	3.9762e + 005	5.7792e + 004	5.2583e + 006	9.3333e + 005	2.1865e + 007	2.8484e + 006
DE/best/1	2.1720e + 004	2.2930e + 004	6.6424e + 008	1.8591e + 008	2.0186e + 010	1.1757e + 009	1.6522e + 011	3.0746e + 010
ABC	318.9369	85.9623	2.7770e + 008	4.6268e + 007	4.1935e + 010	8.4123e + 008	3.5619e + 011	2.6418e + 009
CS	2.3068e + 003	1.6973e + 003	3.8635e + 005	3.0472e + 005	1.0000e + 010	1.1469e + 009	3.1249e + 010	1.362e + 009
CFA	196.9064	0.1282	988.8533	0.1200	4.9485e + 003	0.0	2.4746e + 004	0.0
f_4: Schwefel's function								
PSO	− 3.1530e + 004	3.0160e + 003	− 1.0503e + 005	7.5094e + 003	− 2.7306e + 005	1.7252e + 004	− 4.7175e + 005	4.8773e + 004
DE/best/1	− 5.2755e + 004	1.9128e + 003	− 2.0066e + 005	3.6502e + 003	− 5.0820e + 005	3.3564e + 004	− 1.0181e + 006	193.0189
ABC	− 7.5799e + 004	648.9706	− 2.6139e + 005	3.5172e + 003	− 6.1997e + 005	9.4397e + 003	− 9.7033e + 005	4.4942e + 004
CS	− 4.5570e + 004	336.5017	− 1.2749e + 005	1.5053e + 003	− 2.9566e + 005	3.5152e + 003	− 6.6371e + 005	4.1675e + 003
CFA	− 6.1991e + 004	165.208	− 2.7952e + 005	1.4428e + 003	− 9.1985e + 005	8.2998e + 003	− 2.7160e + 006	1.0271e + 004
f_5: Griewank's function								
PSO	10.5657	2.0449	168.3995	20.0941	1.3081e + 003	93.4573	4.2953e + 003	777.2867
DE/best/1	0.9872	1.1966	3.2882e + 003	163.1826	5.9048e + 004	1.0159e + 003	4.4384e + 005	3.5119e + 004
ABC	3.9883e-004	5.3848e-004	1.8216e + 003	150.2086	9.1194e + 004	1.0966e + 003	6.8171e + 005	2.3373e + 003
CS	10.0966	0.8894	78.2512	3.5176	1.3802e + 003	32.0885	1.1857e + 004	407.5
CFA	0.0	0.0	0.0	0.0	0.0	0.0	0.0	0.0
f_6: Weierstras's function								
PSO	91.9964	1.7222	501.7826	8.4389	2.6052e + 003	47.2272	1.6071e + 004	304.9255
DE/best/1	176.1007	1.1625	1.3246e + 003	5.1093	7.7284e + 003	28.0623	5.5181e + 004	112.6022
ABC	10.3008	0.5803	386.2685	10.5001	3.7878e + 003	103.3638	5.6881e + 004	1.0097e + 003

Table 3 (continued)

Algorithms	D = 200		D = 1000		D = 5000		D = 25,000	
	Mean	Std	Mean	Std	Mean	Std	Mean	Std
CS	116.3462	1.3198	812.9352	10.9190	4.9690e + 003	20.9618	2.8894e + 004	128.5247
CFA	0.0	0.0	0.0	0.0	0.0	0.0	0.0	0.0

large-scale ORPD problems implemented on the standard IEEE 57-, 118-, and 300-bus (large-scale) electrical power grids (Zimmerman et al. 2011). All algorithms have been coded in MATLAB 7.6 software and the simulations were executed on a PC with Pentium IV E5200 CPU and 2 GB RAM configuration. All algorithms have been executed 25 times for each large-scale ORPD problem. The information of the IEEE large-scale power systems is given in Table 5. The number of iterations for all optimization algorithms are set to 500. Furthermore, the permissible limits of the decision variables of all chosen IEEE standard systems are provided in Table 6 (Mouassa et al. 2017; Wang et al. 2014).

5.1 CFA optimizer-based methodology for large-scale ORPD problems

In this sub-section, important aspects of the CFA optimizer when solving large-scale ORPD problems for IEEE 57-, 118-, and 300-bus systems are assessed. The following steps briefly summarizes the CFA optimizer-based large-scale ORPD algorithm:

Step 1 Set initial population size (N), object size (Nob), the maximum number of iterations ($Iter_{max}$), contact probabilistic value (Pc = 0.5), ionization probabilistic value (Pi = 0.1), and input the required information for large-scale systems, including decision variables $u^T = [V_{G1}...V_{\mathrm{GNG}}, Q_{C1}...Q_{\mathrm{CNC}}, T_1...T_{\mathrm{NT}}]$ with generator related constraints, shunt VAr compensator constraints, and transformer tap ratio limitations.

Step 2 Generate the initial randomly solutions matrix (initial population matrix) $[X_0]$ of CFA optimizer based on Eq. 7 and generator, shunt VAr compensator and transformer tap ratio limitations.

Step 3 Calculate the large-scale ORPD objective function F_{ORPD} (Eq. 13) by imposing the the equality (Eq. 6 and Eq. 7) and inequality (Eq. 8 to Eq. 12) constraints for the initial population of CFA optimizer. In this paper, the penalty factors, which are large positive numbers, are used for constraint-handling procedure of the large-scale ORPD, defined based on (Moghadam & Seifi, 2014).

Step 4 Produce new population of CFA optimizer utilizing Eq. 18 through Eq. 20.

Step 5 Calculate the large-scale ORPD objective function values F_{ORPD} (Eq. 13) by imposing the equality (Eq. 6 and Eq. 7) and the inequality (Eq. 8 to Eq. 12) constraints for the new population generated in step 4.

Step 6 In case a new individual outperforms the older one, the latter will be replaced by the former.

Step 7 Generate a new population of the CFA optimizer by ionization and contact probabilistic phase (for multi-

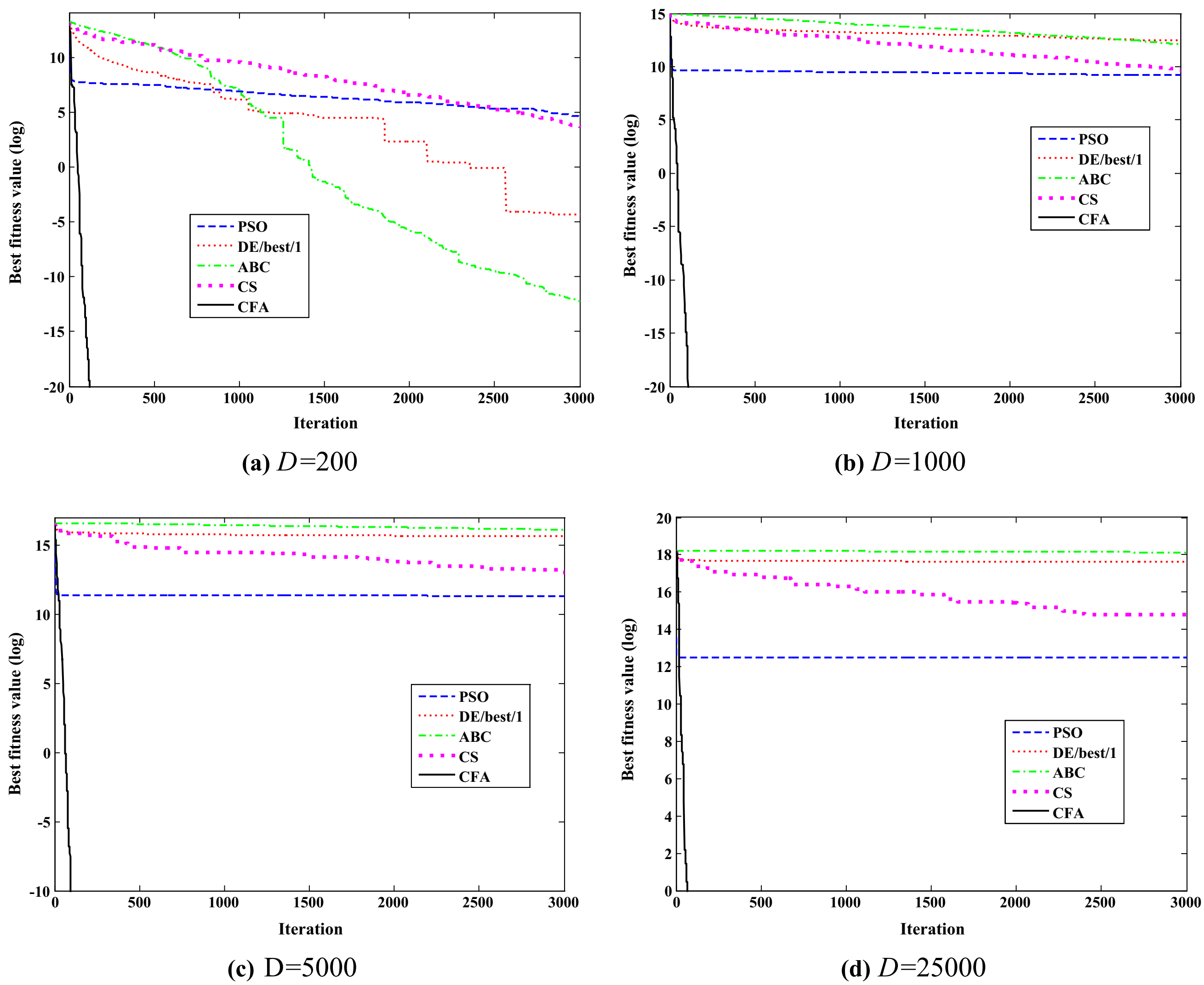

Fig. 3 **a–d** Convergence performance of algorithms for f_1 with different dimensions

Table 4 Solutions of the CFA optimizer when different number of objects (groups) is used for shifted Sphere function

Nob	$D = 200$, $Iter_{max} = 10{,}000$		$D = 600$, $Iter_{max} = 10{,}000$	
	Mean	Std	Mean	Std
1	2.5011e + 005	5.5079e + 003	1.5588e + 006	3.0483e + 004
10	2.0634e + 003	749.5308	3.3058e + 005	1.5264e + 004
20	386.1771	80.0162	1.5294e + 005	2.3230e + 004
40	53.2571	8.5992	7.1244e + 004	1.8974e + 004
200	10.6361	2.7227	6.6095e + 003	479.8862
1000	0.2248	0.0456	2.3539e + 003	5.8321

object CFA optimizer) considering the large-scale ORPD problem constraints.

Step 8 Repeat steps 4–7 of CFA optimizer until reaching $Iter_{max}$ of the CFA optimizer.

5.2 Simulation results for the ORPD problem of large-scale systems

5.2.1 IEEE 57-bus test system

The ORPD problem is solved for the standard IEEE 57-bus system using CFA and other conventional algorithms. Four

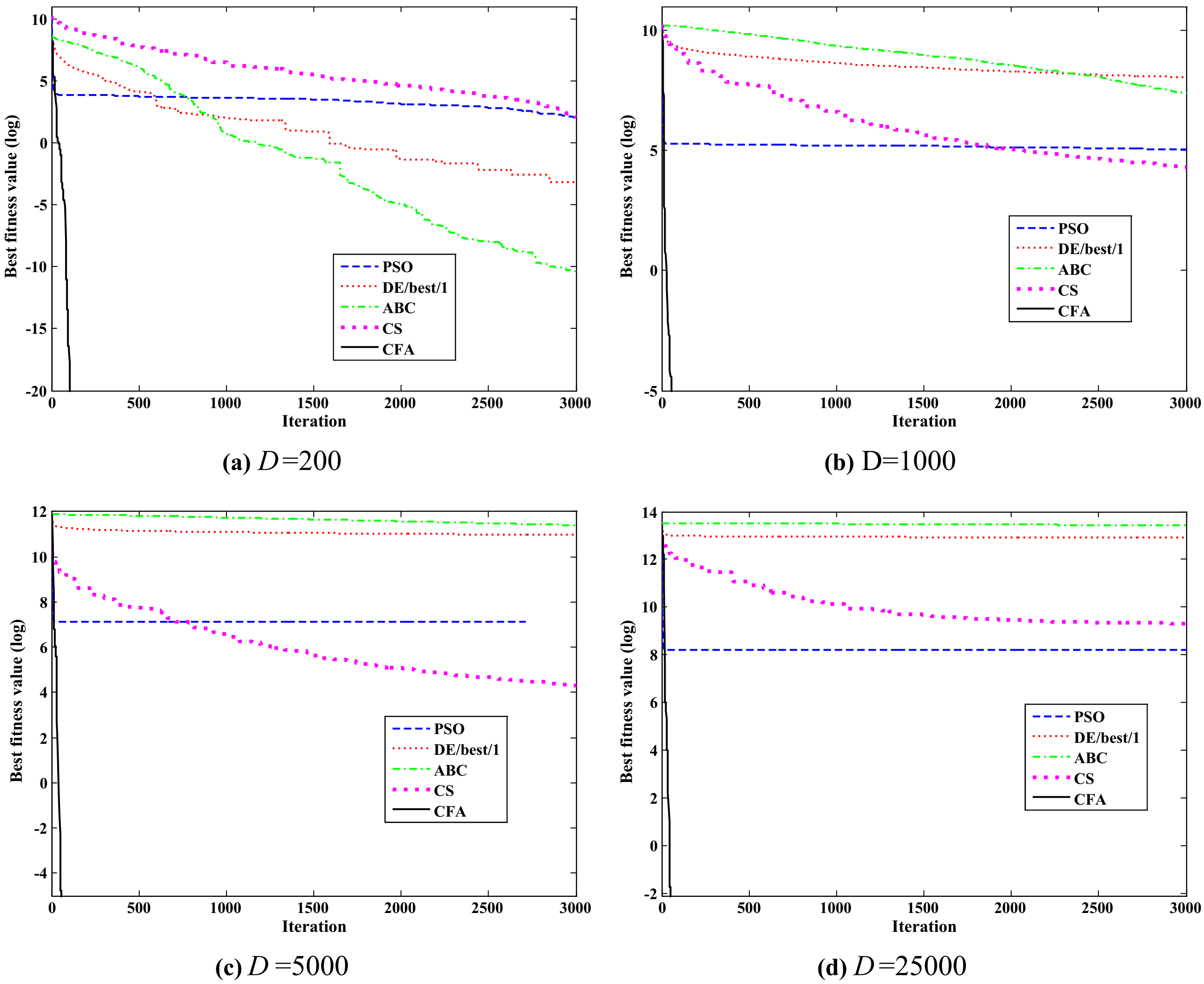

Fig. 4 **a–d** Convergence performance of algorithms for f_5 with different dimensions

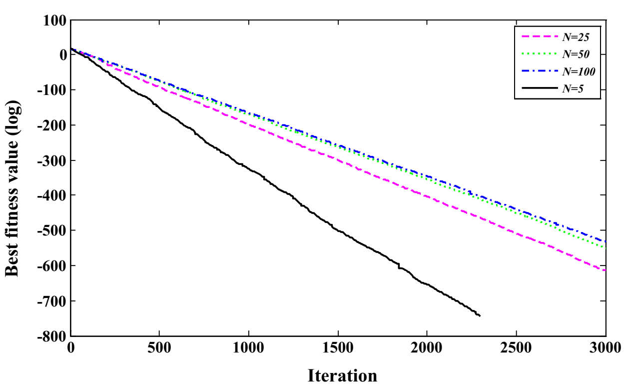

Fig. 5 Convergence rate of CFA optimizer with respect to the population size for Sphere function with D = 25,000

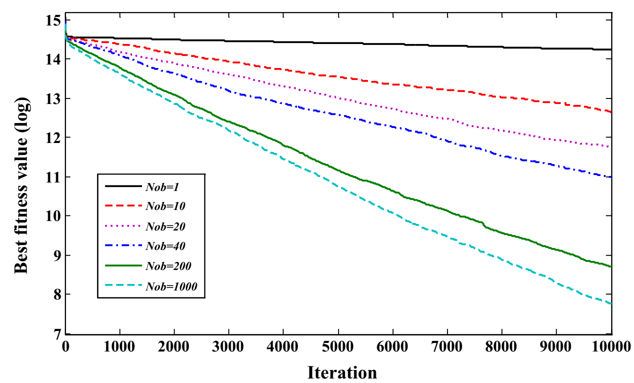

Fig. 6 Convergence graphs of the multi-object CFA optimizer for shifted Sphere function with D = 600 by changing the number of objects

scenarios are defined for solving the resultant ORPD problem based on the population size. To prove that the population size required for CFA is smaller than that of other algorithms, the initial population size for different scenarios is considered to be changed from 5 to 60 members.

Table 5 Description of test systems

Variables	IEEE 57-bus test system	IEEE 118-bus test system	IEEE 300-bus test system
Number of control variables	25	77	190
Number of generators	7	54	69
Number of taps	15	9	107
Number of shunt VAr compensation	3	14	14
Number of branches	80	186	411
Continuous variable	7	54	69
Discrete variable	18	23	121
P0 Loss (MW)	32.512	132.863	408.316

Table 6 Control variables settings for the test systems

Control variables	IEEE 57-bus test system	IEEE 118-bus test system	IEEE 300-bus test system	Step
$V_{Gi}^{\min}$	0.94	0.94	0.9	Continuous
$V_{Gi}^{\max}$	1.06	1.06	1.1	
$T_i^{\min}$	0.9	0.9	0.9	0.01
$T_i^{\max}$	1.1	1.1	1.1	
$Q_{Ci}^{\min}$	See in (Wang et al. 2014)	See in (Wang et al. 2014)	See in (Tang et al. 2013)	1
$Q_{Ci}^{\max}$	See in (Wang et al. 2014)	See in (Wang et al. 2014)	See in (Tang et al. 2013)	

Table 7 Statistical detailed results for IEEE 57-bus test system

N.test	*N*	Algorithm	*Best* (MW)	*Worst* (MW)	*Mean* (MW)	*Std*	Average times (s)
1	30	PSO	30.9438	34.7663	31.558	43.6e + 00	28.15
		DE/best/1	31.1432	39.954	34.8267	65.07e + 00	26.47
		ABC	29.1692	36.2353	31.4132	70.6e + 00	26.81
		CS	29.1442	38.4459	32.279	41.28e + 00	27.63
	5	CFA	**25.0821**	**26.2319**	**25.5745**	**11.29e-02**	**3.16**
2	60	PSO	29.9436	35.3792	31.6956	44.15e + 00	48.22
		DE/best/1	30.1415	34.2353	32.7316	26.84e + 00	44.14
		ABC	28.0228	32.75	30.9732	52.5e + 00	43.8
		CS	29.0936	33.4244	31.3515	31.17e + 00	46.57
	15	CFA	**25.0041**	**25.2122**	**25.1451**	**5.66e-03**	**8.82**
3	120	PSO	29.3118	33.7245	31.2987	16.83e + 00	88.0
		DE/best/1	27.6269	32.4757	29.6462	8.29e + 00	80.19
		ABC	27.6074	32.4628	29.5193	15.75e + 00	79.84
		CS	28.2915	32.3542	29.9384	18.59e + 00	84.65
	30	CFA	**24.5630**	**24.8319**	**24.7743**	**5.78e-03**	**14.22**
4	240	PSO	29.3117	33.5521	31.3962	20.7e + 00	193.24
		DE/best/1	27.6269	32.6903	28.8526	20.61e + 00	172.75
		ABC	27.6074	31.0432	28.8748	2.93e + 00	170.33
		CS	28.0005	31.354	29.3055	14.04e + 00	182.04
	60	CFA	**24.5627**	**24.7271**	**24.5937**	**1.25e-03**	**31.7**

Table 8 Best decision variables settings and active power loss for IEEE 57-bus test system (p.u.)

Variable	IWO (M. Ghasemi et al. 2014a, b, c)	WCA (Heidari et al. 2017)	DMO-ORPD (Mohseni-Bonab et al. 2016a, b)	CFA
V_{G1}	1.06	1.0605	1.013	1.06
V_{G2}	1.05912	1.0602	1.0005	1.05082
V_{G3}	1.04716	1.0497	0.9868	1.04533
V_{G6}	1.03817	1.0018	0.9908	1.04094
V_{G8}	1.05926	1.0600	0.9941	1.05984
V_{G9}	1.02729	1.0589	0.9795	1.02551
V_{G12}	1.0374	1.0538	0.9655	1.03209
$T_{4\text{-}18}$	1.05	0.9923	1.0009	0.96
$T_{4\text{-}18}$	1.0	0.9814	1.0009	0.99
$T_{21\text{-}20}$	1.07	0.9354	0.9844	1.01
$T_{24\text{-}26}$	1.02	0.9953	1.0022	1.01
$T_{7\text{-}29}$	0.97	0.9963	0.9856	0.98
$T_{34\text{-}32}$	0.99	0.9712	0.9519	0.98
$T_{11\text{-}41}$	0.9	0.9865	0.9926	0.9
$T_{15\text{-}45}$	0.96	0.9245	0.9836	0.97
$T_{14\text{-}46}$	0.95	1.0345	1.0076	0.95
$T_{10\text{-}51}$	0.98	1.0056	0.9946	0.96
$T_{13\text{-}49}$	0.93	0.9825	0.9668	0.92
$T_{11\text{-}43}$	0.99	0.9715	0.9000	0.95
$T_{40\text{-}56}$	1.01	0.9923	1.0217	1.02
$T_{39\text{-}57}$	1.04	1.0186	1.0320	0.97
$T_{9\text{-}55}$	0.96	1.0024	1.0025	0.97
Q_{C18}	0.0442	0.0988	0.10	0.10
Q_{C25}	0.0433	0.0590	0.059109	0.059
Q_{C53}	0.0615	0.0629	0.063418	0.063
Ploss	0.245939	0.2482	0.250137	0.245627

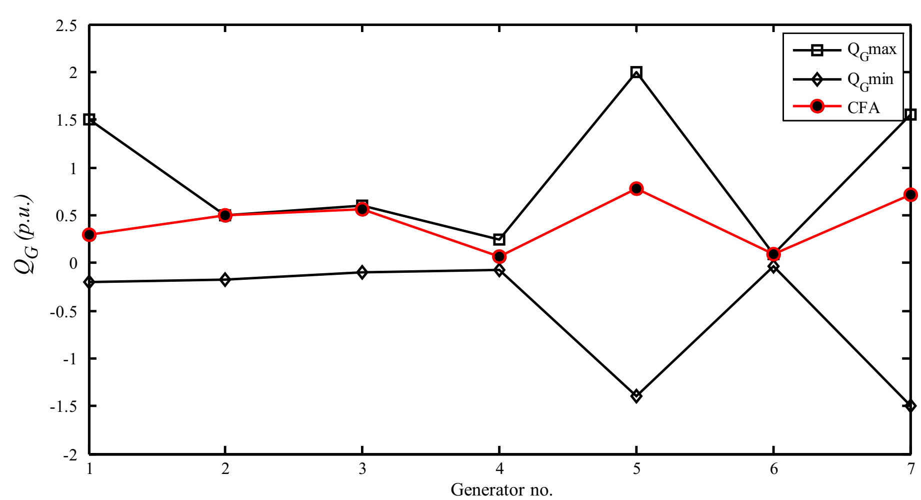

Fig. 7 The constraints of the generated reactive power of generators of the IEEE 57-test system

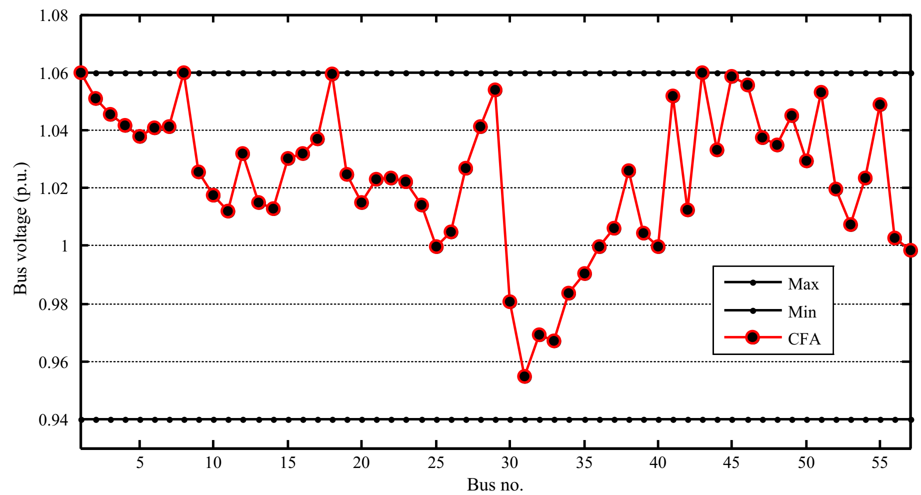

Fig. 8 The constraints of bus voltages of the IEEE 57-bus test system

Table 9 Statistical detailed results for IEEE 118-bus test system

N.test	*N*	Algorithm	*Best* (MW)	*Worst* (MW)	*Mean* (MW)	*Std*	Average times (s)
1	150	PSO	119.0045	146.6439	132.9114	95.72e + 00	254.85
		DE/best/1	119.8516	138.4557	126.1069	31.83e + 00	236.08
		ABC	121.9614	138.0602	127.2836	47.65e + 00	234.97
		CS	120.875	140.747	129.9342	98.54e + 00	248.11
	30	**CFA**	**115.5627**	**118.9382**	**116.8973**	**8.25e-01**	**34.56**
2	300	PSO	118.3369	123.7531	119.9905	37.86e + 00	551.95
		DE/best/1	117.3356	121.7954	119.2183	24.87e + 00	515.74
		ABC	119.2148	126.6823	122.2755	20.63e + 00	510.45
		CS	118.6402	128.8526	124.088	16.19e + 00	537.66
	60	**CFA**	**115.4597**	**116.3178**	**115.9865**	**1.28e-01**	**65.19**
3	600	PSO	116.7624	117.5013	117.1217	6.9e-01	905.92
		DE/best/1	116.9541	118.8652	117.2498	9.16e-01	856.82
		ABC	119.2036	121.4173	120.6704	7.94e + 00	842.6
		CS	117.9885	118.5917	118.735	5.5e + 00	885.93
	90	**CFA**	**114.8262**	**114.9175**	**114.8998**	**9.15e-02**	**82.05**
4	1000	PSO	116.755	119.4836	118.1051	1.21e + 00	1629.46
		DE/best/1	116.7784	117.0018	116.8954	9.37e-01	1386.35
		ABC	118.1923	118.9602	118.349	7.58e-01	1373.57
		CS	117.9761	119.9985	118.9894	1.45e + 00	1464.63
	150	**CFA**	**114.7666**	**114.8412**	**114.8003**	**5.00e-03**	**138.81**

A summary of the results for the best, worst, and average values and the standard deviation (s.t) of results obtained by 25 runs for each algorithm are presented in Table 7. The obtained results, as given in the table, show the performance, strength, and speed of CFA compared to other conventional algorithms.

The proposed method provides a better solution with less deviation and higher convergence rate for each scenario making CFA a strong and powerful algorithm to solve various optimization problems in the power systems. The data presented in Table 7 clearly illustrates that CFA with the population of 60 members reaches a significantly better solution compared to other algorithms (population size of CFA is four times smaller than that of the other algorithms). Furthermore, the final solution obtained by CFA is presented in Table 8 and is compared with several solutions obtained by some recent researches, which obviously demonstrates the superiority of CFA in solving ORPD.

Figures 7 and 8 show the generated reactive power of generators and bus voltages of the IEEE 57-bus test system, respectively, for the best obtained solution by the proposed method. According to these results, as observed, the

Table 10 Best control variables settings (p.u.) for active power loss for IEEE 118-bus test system (p.u.)

Variable	GWO (Sulaiman et al. 2015)	FF (Rajan & Malakar, 2015)	FAHCLPSO (Naderi et al. 2017)	PSOGSA (Radosavljević et al. 2016)	KHA (Mukherjee & Mukherjee, 2016)	NGBWCA (Heidari et al. 2017)	CFA
V_{G1}	1.0204	1.021665	1.0120	1.0299	1.0211	1.0215	1.02714
V_{G4}	1.0257	1.043732	1.0523	1.0598	1.0476	1.0431	1.05817
V_{G6}	1.0208	1.0334	1.0666	1.0529	1.0314	1.0312	1.0506
V_{G8}	1.0419	1.05013	1.0597	0.9888	1.1000	1.0539	1.04007
V_{G10}	1.0413	1.026539	1.0725	0.9408	1.1000	1.0271	1.05734
V_{G12}	1.0232	1.01976	1.0333	1.0508	1.0478	1.0316	1.04744
V_{G15}	1.0207	1.021911	1.0012	1.0235	1.0356	1.0129	1.04655
V_{G18}	1.0270	1.03564	1.0058	1.0211	1.0298	1.0075	1.04926
V_{G19}	1.0204	1.001754	1.1000	1.0187	1.0245	1.0102	1.04538
V_{G24}	1.0137	1.058576	1.0971	1.0231	1.0349	1.0208	1.05185
V_{G25}	1.0270	1.081467	1.0899	1.0281	1.0787	1.0531	1.05993
V_{G26}	1.0386	1.088557	1.1000	1.0599	1.0014	0.9941	1.06
V_{G27}	1.0188	1.059599	1.0654	1.0228	1.0345	1.0291	1.04477
V_{G31}	1.0138	1.030586	1.0318	1.0143	1.0249	1.0275	1.04037
V_{G32}	1.0135	1.051383	1.0322	1.0194	1.0349	1.0201	1.04323
V_{G34}	1.0261	0.985175	0.9999	1.0207	1.0749	1.0014	1.05688
V_{G36}	1.0261	1.043302	0.9998	1.0183	1.0749	1.0412	1.0551
V_{G40}	1.0125	1.009106	1.0501	0.9935	1.0245	1.0400	1.03571
V_{G42}	1.0233	1.014088	1.0231	0.9886	1.0249	1.0512	1.03731
V_{G46}	1.0272	0.986644	1.0005	1.0357	1.0469	1.0170	1.04611
V_{G49}	1.0401	1.045022	0.9897	1.0538	1.0549	1.0510	1.05942
V_{G54}	1.0230	1.044307	0.9998	1.0436	1.0457	1.0392	1.03629
V_{G55}	1.0221	0.999572	1.0222	1.0404	1.0274	1.0331	1.03511
V_{G56}	1.0226	0.994247	1.0008	1.0410	1.0249	1.0372	1.0354
V_{G59}	1.0379	1.047607	1.0731	1.0600	1.0289	1.0564	1.05928
V_{G61}	1.0241	1.030507	1.0258	1.0600	1.0789	1.0565	1.06
V_{G62}	1.0199	1.03358	1.0059	1.0566	1.0659	1.0489	1.05604
V_{G65}	1.0465	1.06538	1.0630	1.0239	1.0991	1.0435	1.06
V_{G66}	1.0378	1.028989	1.0312	1.0600	1.0451	1.0435	1.06
V_{G69}	1.0501	1.046139	1.0636	1.0600	1.0359	1.0489	1.06
V_{G70}	1.0243	1.07727	1.1000	1.0350	1.0542	1.0113	1.03518
V_{G72}	1.0187	1.022816	1.0500	1.0302	1.0511	1.0382	1.04059
V_{G73}	1.0397	1.031771	1.0981	1.0587	1.0459	0.9926	1.0351
V_{G74}	1.0170	1.030611	1.0444	1.0066	1.0359	0.9934	1.02239
V_{G76}	1.0080	1.015462	1.0037	0.9957	1.0259	1.0324	1.00482
V_{G77}	1.0192	1.051973	1.0559	1.0382	1.0280	1.0185	1.04569
V_{G80}	1.0329	1.039807	0.9999	1.0542	1.0421	1.0021	1.05981
V_{G85}	1.0224	1.077938	1.0882	1.0446	1.0353	1.0312	1.05103
V_{G87}	1.0361	1.002763	1.0303	1.0515	1.0963	1.0212	1.05786
V_{G89}	1.0558	1.074747	1.0001	1.0600	1.0759	1.0387	1.06
V_{G90}	1.029	1.047818	1.0018	1.0323	1.0425	1.0071	1.04222
V_{G91}	1.0127	1.048983	1.0298	1.0273	1.0358	0.9989	1.04552
V_{G92}	1.036	1.047601	1.1005	1.0431	1.0516	1.0001	1.0485
V_{G99}	1.0297	1.042693	1.0498	1.0072	1.0415	1.0467	1.05421
V_{G100}	1.036	1.038511	1.0565	1.0522	1.0426	1.0213	1.05881
V_{G103}	1.0232	1.022228	1.0413	1.0480	1.0220	1.0416	1.04916
V_{G104}	1.018	1.03061	1.0189	1.0353	1.0041	1.0174	1.03833

Table 10 (continued)

Variable	GWO (Sulaiman et al. 2015)	FF (Rajan & Malakar, 2015)	FAHCLPSO (Naderi et al. 2017)	PSOGSA (Radosavljević et al. 2016)	KHA (Mukherjee & Mukherjee, 2016)	NGBWCA (Heidari et al. 2017)	CFA
V_{G105}	1.0176	1.053364	1.1000	1.0339	1.0147	1.0223	1.03531
V_{G107}	1.0201	1.014579	1.0222	1.0422	0.9879	1.0340	1.02247
V_{G110}	1.0207	1.034131	1.0115	1.0196	1.0120	1.0103	1.03178
V_{G111}	1.0261	1.031144	1.1000	1.0270	1.0258	1.0345	1.03948
V_{G112}	1.0066	1.011916	1.0500	1.0015	0.9928	1.0160	1.01614
V_{G113}	1.0251	1.021931	1.0099	1.0337	1.0415	1.0181	1.0554
V_{G116}	1.0342	1.053512	1.0500	1.0067	1.0254	1.0330	1.05743
$T_{5\text{-}8}$	1.0208	1.002155	1.0214	0.9182	1.0740	1.0051	0.98
$T_{25\text{-}26}$	1.0279	0.941079	1.0533	1.1000	1.0245	0.9614	1.06
$T_{17\text{-}30}$	1.0323	0.974903	1.0555	0.9790	1.0456	0.9961	0.98
$T_{37\text{-}38}$	1.0209	0.989385	0.9995	0.9759	0.9874	0.9523	0.99
$T_{59\text{-}63}$	1.0091	0.992515	1.0619	0.9000	1.0389	1.0521	0.98
$T_{61\text{-}64}$	1.0366	0.98305	1.0318	0.9287	1.0147	0.9520	1.00
$T_{65\text{-}66}$	1.0301	0.971375	1.0490	1.0057	0.9245	0.9812	0.99
$T_{68\text{-}69}$	1.0234	0.936734	0.9660	0.9715	0.9945	0.9510	0.95
$T_{80\text{-}81}$	1.0211	0.979664	0.9732	0.9459	1.0780	0.9754	0.99
Q_{C5}	− 39.76	0.0	0.3500	− 33.5074	0.3979	− 0.0723	− 19.92
Q_{C34}	13.79	2.389537	10.1922	7.6243	0.0005	0.0483	7.47
Q_{C37}	− 24.73	0.0	1.7500	− 19.7317	0.2389	− 0.2390	− 5.06
Q_{C44}	9.9571	6.471033	4.4000	6.5258	0.0009	0.0032	4.46
Q_{C45}	9.8678	5.015351	6.9894	4.5300	0.0489	0.0372	1.63
Q_{C46}	9.9186	1.108324	7.1289	3.1784	0.0002	0.0624	9.55
Q_{C48}	14.89	6.989812	6.6668	11.8388	0.0005	0.0172	3.35
Q_{C74}	11.972	7.310902	11.0952	3.8061	0.0003	0.0013	0.0
Q_{C79}	19.649	9.132848	15.0000	13.9863	0.0008	0.0621	0.0
Q_{C82}	19.89	9.882076	10.5509	17.7504	0.0419	0.0463	0.0
Q_{C83}	9.9515	6.716357	5.5540	1.9938	0.0500	0.0560	0.0
Q_{C105}	19.968	10.66619	15.1895	6.8200	0.0010	0.0653	4.65
Q_{C107}	5.9136	4.262622	4.4140	6.0000	0.0076	0.0072	4.19
Q_{C110}	5.8834	2.402687	2.2310	4.4194	0.0222	0.0108	2.25
Ploss	120.65	135.42	116.2479	122.4709	118.85	121.47	114.7666

constraints of the ORPD problem have suitably been satisfied and thus the obtained results are acceptable.

5.2.2 IEEE 118-bus test system

In order to show the accuracy and performance of the proposed method for large-scale power systems, the CFA-optimizer is applied to solve the ORPD problem formulated for the IEEE 118-bus system. The same scenarios as presented in the previous sub-section are considered for the 118-bus system as well. The conditions for all algorithms are identical except the population size of CFA. Table 9 presents the statistical data obtained from 25 independent runs for all algorithms. According to the results given in this table, the proposed method provides a better performance as the problem becomes larger. For small population size, the results obtained by the proposed method are in an acceptable range, and when the population size increases from 30 to 150, the results do not noticeably change in comparison to those of other methods; this improves the run time (computational cost) of the proposed CFA to solve ORPD. Moreover, the best solution obtained by CFA optimizer and some other conventional methods are given in Table 10. One can observe that the proposed method provides a better solution in comparison to some other recently proposed algorithms.

Furthermore, constraints pertinent to the output reactive power of generators and bus voltage magnitudes, which are

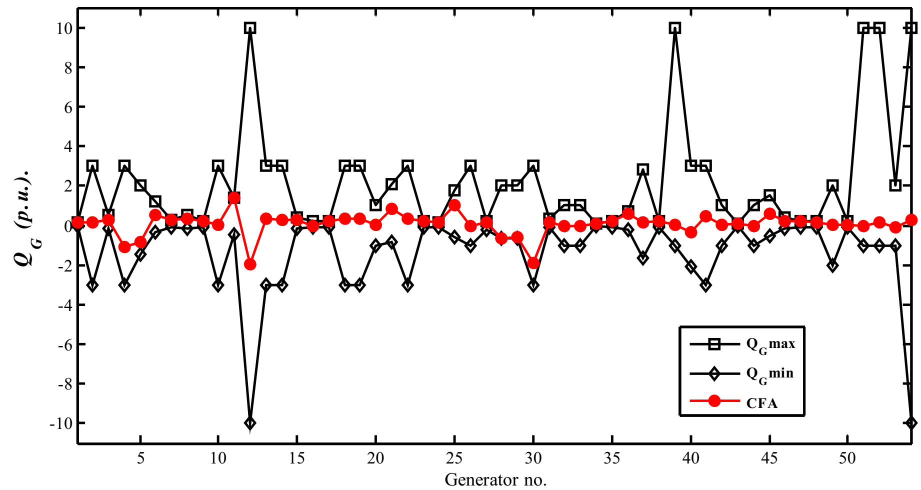

Fig. 9 The constraints of the generated reactive power of generators of the IEEE 118-bus test system

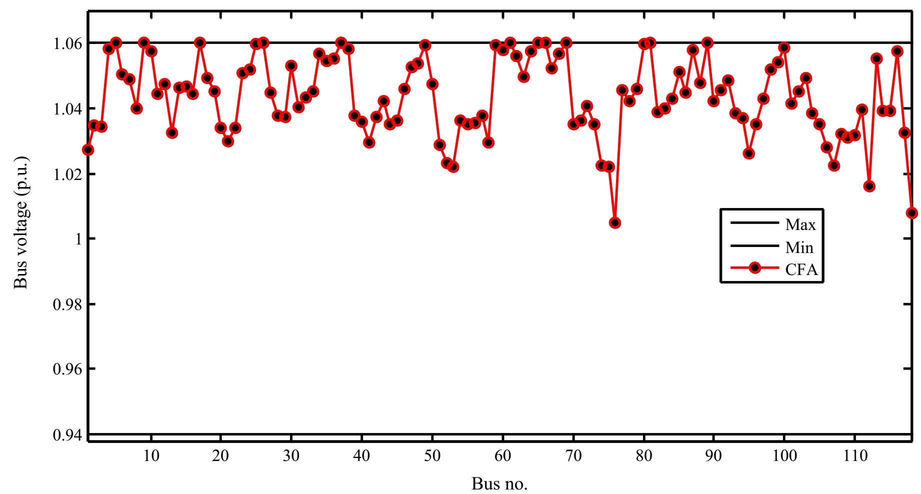

Fig. 10 The constraints of bus voltage magnitudes of the IEEE 118-bus test system

Table 11 Statistical details for IEEE 300-bus test system

N.test	*N*	Algorithm	*Best* (MW)	*Worst* (MW)	*Mean* (MW)	*Std*	Average times (s)
1	300	PSO	398.2514	448.2514	425.5109	5.25e + 02	5634.5
		DE/best/1	403.7391	433.8953	412.2768	4.63e + 02	4091.2
		ABC	401.1106	441.5629	417.4354	3.12e + 02	3886.8
		CS	402.0142	435.4376	415.9743	7.45e + 02	4706.6
	60	**CFA**	**377.2348**	**381.9188**	**379.0071**	**1.48e + 00**	**265.4**
2	450	PSO	398.6379	442.9142	424.7488	3.71e + 02	8768.2
		DE/best/1	397.405	405.3868	400.5007	2.46e + 02	6107.9
		ABC	395.1445	422.5629	413.62	2.00e + 02	5940.0
		CS	400.0142	430.8965	412.6103	1.83e + 02	7643.9
	120	**CFA**	**375.1659**	**379.825**	**377.4413**	**8.75e-01**	**600.3**
3	600	PSO	390.5690	427.1685	414.9492	8.26e + 01	12,650.7
		DE/best/1	387.2168	406.1	396.1453	1.71e + 01	9120.6
		ABC	392.753	419.9766	410.5515	2.68e + 01	8269.1
		CS	394.8636	430.4049	410.3805	3.13e + 01	11,006.3
	240	**CFA**	**375.0025**	**377.4539**	**376.1123**	**6.81e-02**	**1140.7**

Table 12 Comparison of CFA optimizer with the recently proposed methods in the literature for IEEE 300-bus system

	ALO (Mouassa et al. 2017)	A-CSOS (Yalçın et al. 2019)	CFA
Losses *Best* (MW)	384.9224	380.5328	375.0025
Average times (s)	4022.9	–	1140.7

two main constraints of the problem, are given in Figs. 9 and 10, respectively. As observed, the final solution fully satisfies the constraints meaning that the obtained optimal solution is feasible.

5.2.3 IEEE 300-bus test system

The last test system investigated in this paper is the IEEE standard 300-bus system, which is considered as a very large-scale test system. All scenarios are assumed to be similar to those presented in the above sub-sections under identical conditions. A summary of the results obtained by all algorithms for ORPD problem is given in Table 11. Similar to the previous sub-sections, the proposed CFA significantly performs better than the other algorithms. Furthermore, Table 12 presents the results obtained by CFA compared to those of recent studies, demonstrating the supremacy of the method presented in this paper.

6 An early attempt for improving CFA optimizer

In this section, as an early attempt for improving CFA optimizer, various relationships are tested for the CFA's attraction/repulsion phase to select the best relationship to increase the efficiency of this algorithm. For this purpose, in relation (18), instead of using 2 as the powers of |cosθ| and |sinθ|, P_1 and P_2 are used, respectively, as follows:

$$x_j^{\text{new}} = x_j^{\text{old}} + \left|\cos\theta_j^{\text{new}}\right|^{p_1} \times \left(x^{\text{Best}} - x^{\text{Worst}}\right) + \left|\sin\theta_j^{\text{new}}\right|^{p_2} \times \left(\text{mean}\left(\sum_{m=1\in \text{Ob}_i}^{\alpha,\alpha\le\alpha_{\max}} x_m^{\text{Better}-\text{than}-\text{x}_j}\right) - \text{mean}\left(\sum_{m=1\in \text{Ob}_i}^{r,r\le r_{\max}} x_m^{\text{Worse}-\text{than}-\text{x}_j}\right)\right) \tag{21}$$

For this supplementary study, 14 test functions of CEC 2005 (f_1 to f_{14}) (Suganthan et al. 2005) which have been successfully implemented in many papers, are selected. The population and the number of iterations of the algorithm are set to be 20 and 15,000, respectively, giving the number of the objective function evaluations (FEs) equal to 300,000.

Tables 13 and 14 show the mean and the standard deviation of the results obtained from the different versions of CFA for these functions, respectively. In Table 13, the solutions that are better than the original version are shown in boldface. Based on these results, it can be said that using the values $p_1 = 2 * |Sin(\theta)|$ and $p_2 = 2 * |Cos(\theta)|$ are the best choice for CFA. The convergence characteristics of different versions of CFA for some of the test functions are shown in Fig. 11.

Tables 15 and 16 demonstrate the results obtained from different versions of CFA optimizer in solving the ORPD problems in 118- and 300-bus test systems, respectively. The selected conditions for the algorithms are the same as the original conditions given in the article. It can be seen that the new version with $p_1 = 2 * |Sin(\theta)|$ and $p_2 = 2 * |Cos(\theta)|$ has achieved a better solution than other versions of CFA.

According to the studies, it is clear that the new version with $p_1 = 2 * |Sin(\theta)|$ and $p_2 = 2 * |Cos(\theta)|$ is much better and more suitable than the original version for the real-world optimization.

7 Conclusions

An efficient algorithm, referred to as the CFA optimizer, is presented in this paper. The aim of the current work is to explore and find global solutions of various high-dimensional ORPD problems of large-scale power systems including the IEEE standard 57-, 118-, and 300-bus test systems. In order to assess the efficiency and optimization power of the CFA optimizer, a comparison was made between the results of the proposed method and other algorithms for high-dimensional optimization problems. The simulation results demonstrate that the proposed CFA optimizer is able to provide the global optimal solution of many different types of high-dimensional test functions and ORPD problems. Finally, an early attempt was carried out for reaching a more powerful CFA optimizer, in which the proposed modified versions were tested on benchmark and ORPD problems. The simple study shows that the optimization efficiency of CFA can be further improved using some simple modifications. The more thorough investigations about the best modifications to be done for improving CFA optimizer can be the subject of future

Table 13 Mean of the results obtained by different versions of CFA for the real-parameter unimodal and multimodal test functions

P1	—	Original (2)	2	sinθ	sinθ	|sinθ|	2*|sinθ|	|sinθ| +|cosθ|
P2	—	Original (2)	cosθ	2	cosθ	|cosθ|	2*|cosθ|	|sinθ| +|cosθ|
Test functions		Mean	Mean	Mean	Mean	Mean	Mean	Mean
Unimodal Functions	f_1	0.027424970268	40.2391410444	**0.018710007207**	23.6530857582	0.50669019304	**0.014020653593**	0.30420008009
	f_2	54.666922309	1410.91398563	89.748266533	1492.24718854	215.52629576	82.448027341	218.99795044
	f_3	5,744,318.0667	17,641,616.2589	**5,010,549.3607**	16,518,082.7487	8,748,017.6817	5,964,352.5232	6,851,291.0796
	f_4	321.90842771	1130.63160071	393.17731993	1384.61466391	473.96725217	**268.64804258**	368.37315422
	f_5	8750.9177566	10,151.5188846	**7950.8732209**	10,582.1206412	**8319.3599354**	9267.3290824	9446.7726219
Basic Multimodal Functions	f_6	1571.1514314	26,281.2180412	2143.0649711	26,737.1388794	**1343.0343181**	**1401.8360234**	4178.4761286
	f_7	1.0086622648	4.99111267365	1.0748946741	6.32416153764	1.4480029542	**0.96445128044**	1.2814822929
	f_8	20.713184804	20.8734287668	20.778213836	20.8106244564	20.823373004	**20.689366744**	20.826049042
	f_9	30.608112821	88.8090952685	**28.612310683**	79.8003600165	67.096845658	34.114862553	44.683109544
	f_{10}	244.43489966	**168.856428038**	303.75841104	**175.191505385**	**228.10636252**	258.24305593	**221.97940701**
	f_{11}	31.318280423	**31.8154981345**	33.763579467	31.5031059748	**30.469268672**	**31.249426383**	**30.197663332**
	f_{12}	16,118.639533	49,089.3096394	19,442.152716	47,802.5417302	28,210.054868	**8807.0039251**	24,612.718448
Expanded Multimodal Functions	f_{13}	4.27	10.72	**3.65**	9.65	5.22	**3.46**	6.18
	f_{14}	12.96	**12.95**	**12.90**	13.05	**12.81**	12.96	**12.92**
±/=		#/#/#	3/11/0	6/8/0	1/13/0	5/9/0	**8/5/1**	3/11/0

Table 14 Standard deviation of the results obtained by different versions of CFA for the real-parameter unimodal and multimodal test functions

P1	—	Original (2)	2	sinθ	sinθ	|sinθ|	2*|sinθ|	|sinθ| +|cosθ|
P2	—	Original (2)	cosθ	2	cosθ	|cosθ|	2*|cosθ|	|sinθ| +|cosθ|
Test functions		Std	Std	Std	Std	Std	Std	Std
Unimodal Functions	f_1	0.013141461087	43.178111493	0.017839193676	5.7482594539	0.29784435974	0.00704911541	0.097325644352
	f_2	23.289137713	746.85284545	36.680514231	1135.2627681	118.40062619	36.67565527	116.87913988
	f_3	1,854,348.1329	9,452,185.7964	3,090,181.6207	4,625,011.7656	3,390,148.1865	2,114,972.8623	2,630,861.0543
	f_4	332.10425567	492.08573032	215.58511276	941.99230321	241.28958754	144.77256475	197.30024165
	f_5	2500.2268267	1894.4625815	2577.8787925	2744.6127205	1598.9813391	1874.3187779	2809.1275622
Basic Multimodal Functions	f_6	2316.7640577	12,485.354153	2496.1771636	30,656.324655	1397.3763231	3446.044563	5496.8795914
	f_7	0.11667309409	1.719484307	0.047187240965	3.1448172202	0.18334814729	0.13625980879	0.16883069774
	f_8	0.087117973486	0.063374393878	0.11005117644	0.057989368977	0.083797657781	0.082192982139	0.054330901305
	f_9	10.95074716	21.958033731	9.3413238699	24.642717922	17.708766911	19.51983672	8.8708797143
	f_{10}	66.270523985	48.619405703	86.957146663	23.952969127	55.980338589	89.862296978	42.637483224
	f_{11}	2.7458201013	2.2517596426	1.9717490587	3.2660175147	2.5598082774	3.2851998576	2.4511032748
	f_{12}	12,450.851322	23,910.775809	8657.4967243	16,167.061085	15,924.235465	4610.6098608	15,760.186666
Expanded Multimodal Functions	f_{13}	0.80322858407	2.4039115623	1.0530175033	2.4728129407	1.7341633492	0.9469871701	2.186228797
	f_{14}	0.42156496772	0.36454984524	0.48864138263	0.41051485683	0.48647707287	0.3402008448	0.38229412457
± / =			3/11/0	6/8/0	1/13/0	5/9/0	8/5/1	

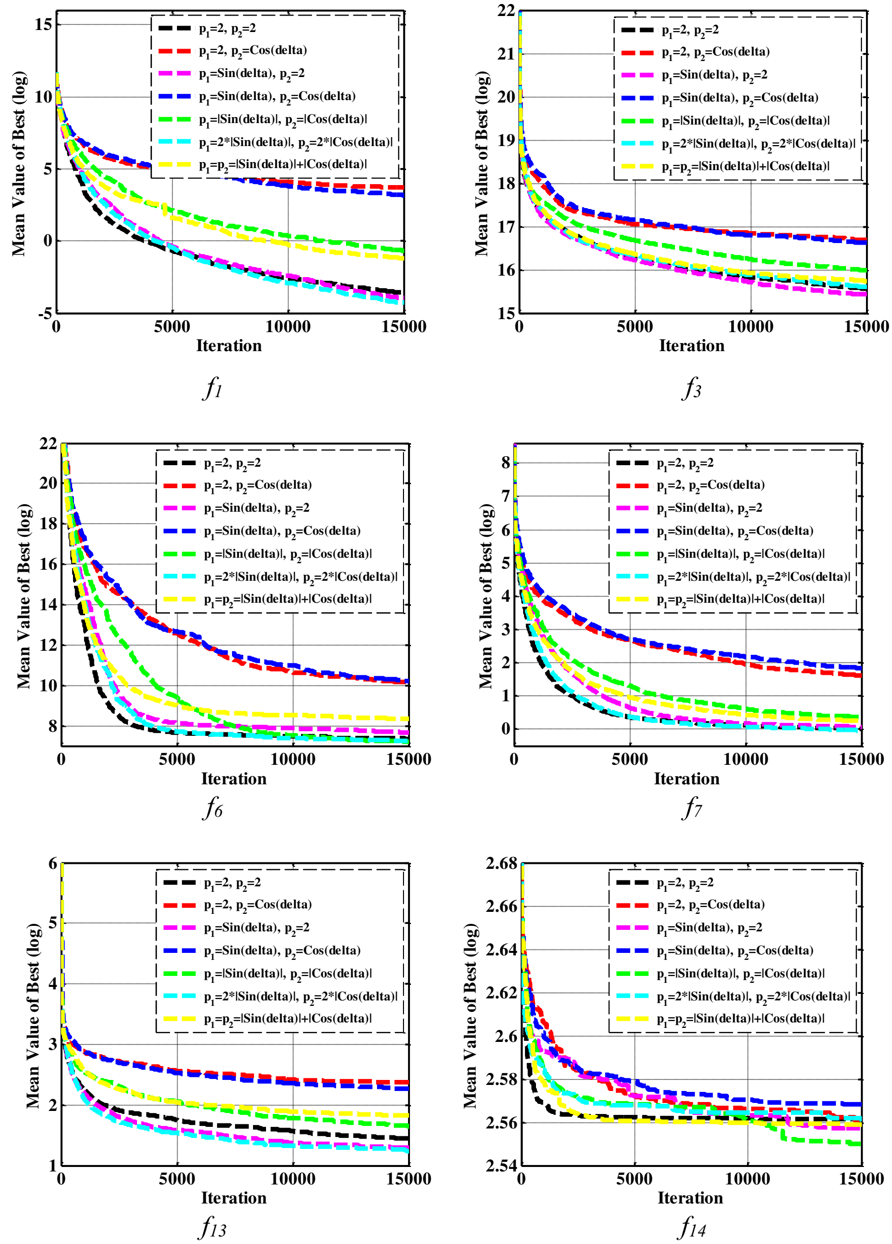

Fig. 11 Convergence characteristics of different versions of CFA for test functions f_1, f_3, f_6, f_7, f_{13} and f_{14}

Table 15 Comparison of the ORPD solutions obtained by different versions of CFA optimizer for IEEE 118-bus system

p_1	p_2	Best (MW)	Worst (MW)	Mean (MW)	Std
2	**2**	**114.7666**	**114.8412**	114.8003	5.00e-03
2	Cosθ	115.1705	118.2524	116.8162	3.15e + 00
Sinθ	2	114.7672	114.8605	114.8148	4.08e-03
Sinθ	Cosθ	115.2294	117.4593	116.7465	1.90 + 00
|Sinθ|	|Cosθ|	114.7769	116.9315	115.9937	9.46e-01
2 $*$ |Sinθ|	2 $*$ |Cosθ|	**114.7666**	114.8415	**114.7978**	**3.52e-03**
|Sinθ| + |Cosθ|	|Sinθ| + |Cosθ|	114.7745	115.0021	114.8926	8.34e-02

Table 16 Comparison of the ORPD solutions obtained by different versions of CFA optimizer for IEEE 300-bus system

p_1	p_2	Best (MW)	Worst (MW)	Mean (MW)	Std
2	**2**	375.0025	**377.4539**	376.1123	6.81e-02
2	Cosθ	377.2394	395.6621	385.2983	1.83e + 01
Sinθ	2	375.1147	378.3216	376.4450	9.90e-02
Sinθ	Cosθ	376.8488	396.1376	388.9714	1.75e + 01
|Sinθ|	|Cosθ|	376.0943	383.5117	377.2983	8.42e + 00
2 $*$ |Sinθ|	2 $*$ |Cosθ|	**374.6825**	377.7053	**375.8190**	**5.22e-02**
|Sinθ| + |Cosθ|	|Sinθ| + |Cosθ|	375.0025	380.5692	378.0648	3.34e + 00

studies. Furthermore, the proposed improved CFA optimizer can be applied for solving other real-world and engineering optimization problems.

Funding The authors have not disclosed any funding.

Data availability Enquiries about data availability should be directed to the authors.

Declarations

Conflict of interest The authors declare that they have no conflict of interest.

Ethical approval This article does not contain any studies with human participants or animals performed by any of the authors.

References

Abido MA (2006) Multiobjective Optimal VAR Dispatch Using Strength Pareto Evolutionary Algorithm. In: 2006 IEEE International Conference on Evolutionary Computation.https://doi.org/10.1109/cec.2006.1688384

Amrane Y, Boudour M, Belazzoug M (2015) A new optimal reactive power planning based on differential search algorithm. Int J Electr Power Energy Syst 64:551–561. https://doi.org/10.1016/j.ijepes.2014.07.060

Atashpaz-Gargari E, Lucas C (2007) Imperialist competitive algorithm: an algorithm for optimization inspired by imperialistic competition. IEEE Congr Evolut Comput 2007:4661–4667. https://doi.org/10.1109/CEC.2007.4425083

Azzam M, Mousa AA (2010) Using genetic algorithm and TOPSIS technique for multiobjective reactive power compensation. Electr Power Syst Res 80(6):675–681. https://doi.org/10.1016/j.epsr.2009.10.033

Basu M (2016) Multi-objective optimal reactive power dispatch using multi-objective differential evolution. Int J Electr Power Energy Syst 82:213–224. https://doi.org/10.1016/j.ijepes.2016.03.024

Bhattacharyya B, Kumar S (2015) Reactive power planning with FACTS devices using gravitational search algorithm. Ain Shams Eng J 6(3):865–871. https://doi.org/10.1016/j.asej.2015.02.002

Bhattacharyya B, Raj S (2016) PSO based bio inspired algorithms for reactive power planning. Int J Electr Power Energy Syst 74:396–402. https://doi.org/10.1016/j.ijepes.2015.07.037

Chen G, Liu L, Zhang Z, Huang S (2017) Optimal reactive power dispatch by improved GSA-based algorithm with the novel strategies to handle constraints. Appl Soft Comput 50:58–70. https://doi.org/10.1016/j.asoc.2016.11.008

Cheng R, Jin Y (2015) A competitive swarm optimizer for large scale optimization. IEEE Trans Cybern 45(2):191–204. https://doi.org/10.1109/tcyb.2014.2322602

Chowdhury A, Liu H, McCalley JD, Krishnan V (2014) Optimal planning of static and dynamic reactive power resources. IET Gener Transm Distrib 8(12):1916–1927. https://doi.org/10.1049/iet-gtd.2014.0081

Chung CY, Liang CH, Wong KP, Duan XZ (2010) Hybrid algorithm of differential evolution and evolutionary programming for optimal reactive power flow. IET Gener Transm Distrib 4(1):84. https://doi.org/10.1049/iet-gtd.2009.0007

Dai C, Chen W, Zhu Y, Zhang X, Dai C, Chen W, Zhu Y, Zhang X (2009) Seeker optimization algorithm for optimal reactive power dispatch. IEEE Trans Power Syst 24(3):1218–1231. https://doi.org/10.1109/tpwrs.2009.2021226

de Sousa VA, Baptista EC, da Costa GRM (2009) Loss minimization by the predictor–corrector modified barrier approach. Electr Power Syst Res 79(5):803–808. https://doi.org/10.1016/j.epsr.2008.10.014

de Souza ACZ, Leme R, Lo KLL, de Souza JCS, Almeida ABB, Zambroni de Souza AC, Leme R, Lo KLL, Stacchini de Souza JC, Almeida ABB (2012) Reactive power redispatch for loss reduction using a modified power flow Jacobian. IET Gener Transm Distrib 6(7):657. https://doi.org/10.1049/iet-gtd.2011.0685

Deeb N, Shahidehpour SM (1990) Linear reactive power optimization in a large power network using the decomposition approach. IEEE Trans Power Syst 5(2):428–438. https://doi.org/10.1109/59.54549

Duman S, Sönmez Y, Güvenç U, Yörükeren N (2012) Optimal reactive power dispatch using a gravitational search algorithm. IET Gener Transm Distrib 6(6):563. https://doi.org/10.1049/iet-gtd.2011.0681

Eberhart R, Kennedy J (1995) A new optimizer using particle swarm theory. In: MHS'95. Proceedings of the Sixth International Symposium on Micro Machine and Human Science. IEEE. https://doi.org/10.1109/mhs.1995.494215

El Ela AAA, Abido MA, Spea SR (2011) Differential evolution algorithm for optimal reactive power dispatch. Electr Power Syst Res 81(2):458–464. https://doi.org/10.1016/j.epsr.2010.10.005

Ghasemi A, Valipour K, Tohidi A (2014a) Multi objective optimal reactive power dispatch using a new multi objective strategy. Int J Electr Power Energy Syst 57:318–334. https://doi.org/10.1016/j.ijepes.2013.11.049

Ghasemi M, Ghanbarian MM, Ghavidel S, Rahmani S, Mahboubi Moghaddam E (2014b) Modified teaching learning algorithm and double differential evolution algorithm for optimal reactive power dispatch problem: a comparative study. Inf Sci 278:231–249. https://doi.org/10.1016/j.ins.2014.03.050

Ghasemi M, Ghavidel S, Ghanbarian MM, Habibi A (2014c) A new hybrid algorithm for optimal reactive power dispatch problem with discrete and continuous control variables. Appl Soft Comput 22:126–140. https://doi.org/10.1016/j.asoc.2014.05.006

Ghasemi M, Taghizadeh M, Ghavidel S, Aghaei J, Abbasian A (2015) Solving optimal reactive power dispatch problem using a novel teaching–learning-based optimization algorithm. Eng Appl Artif Intell 39:100–108. https://doi.org/10.1016/j.engappai.2014.12.001

Ghasemi M, Ghavidel S, Aghaei J, Akbari E, Li L (2018) CFA optimizer: A new and powerful algorithm inspired by Franklin's and Coulomb's laws theory for solving the economic load dispatch problems. Int Trans Electr Energy Syst 28(5):e2536. https://doi.org/10.1002/etep.2536

Heidari AA, Ali Abbaspour R, Rezaee Jordehi A (2017) Gaussian bare-bones water cycle algorithm for optimal reactive power dispatch in electrical power systems. Appl Soft Comput 57:657–671. https://doi.org/10.1016/j.asoc.2017.04.048

Hongxin L, Yinhong L, Jinfu C (2013) Adaptive multiple evolutionary algorithms search for multi-objective optimal reactive power dispatch. Int Trans Electr Energy Syst 24(6):780–795. https://doi.org/10.1002/etep.1730

Hong-Zhong L, Hao-Zhong C, Zheng Y (2010) A novel reactive power planning method based on improved particle swarm optimization with static voltage stability. Eur Trans Electr Power 20(8):1129–1137. https://doi.org/10.1002/etep.389

Hosseini HS (2007) Problem solving by intelligent water drops. In: 2007 IEEE Congress on Evolutionary Computation. https://doi.org/10.1109/cec.2007.4424885

Huang C-M, Chen S-J, Huang Y-C, Yang H-T (2012) Comparative study of evolutionary computation methods for active-reactive power dispatch. IET Gener Transm Distrib 6(7):636. https://doi.org/10.1049/iet-gtd.2011.0559

Jeyadevi S, Baskar S, Babulal CK, Willjuice Iruthayarajan M (2011) Solving multiobjective optimal reactive power dispatch using modified NSGA-II. Int J Electr Power Energy Syst 33(2):219–228. https://doi.org/10.1016/j.ijepes.2010.08.017

Kanna B, Singh SN (2015) Towards reactive power dispatch within a wind farm using hybrid PSO. Int J Electr Power Energy Syst 69:232–240. https://doi.org/10.1016/j.ijepes.2015.01.021

Karaboga D, Basturk B (2007) A powerful and efficient algorithm for numerical function optimization: artificial bee colony (ABC) algorithm. J Global Optim 39(3):459–471. https://doi.org/10.1007/s10898-007-9149-x

Khazali AH, Kalantar M (2011) Optimal reactive power dispatch based on harmony search algorithm. Int J Electr Power Energy Syst 33(3):684–692. https://doi.org/10.1016/j.ijepes.2010.11.018

Khorsandi A, Alimardani A, Vahidi B, Hosseinian SHH (2011) Hybrid shuffled frog leaping algorithm and Nelder-Mead simplex search for optimal reactive power dispatch. IET Gener Transm Distrib 5(2):249. https://doi.org/10.1049/iet-gtd.2010.0256

Li Y, Li X, Li Z (2017) Reactive power optimization using hybrid CABC-DE algorithm. Electr Power Compon Syst 45(9):980–989. https://doi.org/10.1080/15325008.2017.1311387

Liang CH, Chung CY, Wong KP, Duan XZ, Tse CT (2007) Study of differential evolution for optimal reactive power flow. IET Gener Transm Distrib 1(2):253. https://doi.org/10.1049/iet-gtd:20060123

Lopez JC, Contreras J, Munoz JI, Mantovani JRS (2013) A multi-stage stochastic non-linear model for reactive power planning under contingencies. IEEE Trans Power Syst 28(2):1503–1514. https://doi.org/10.1109/TPWRS.2012.2226250

Mahadevan K, Kannan PS (2010) Comprehensive learning particle swarm optimization for reactive power dispatch. Appl Soft Comput 10(2):641–652. https://doi.org/10.1016/j.asoc.2009.08.038

Mallipeddi R, Jeyadevi S, Suganthan PN, Baskar S (2012) Efficient constraint handling for optimal reactive power dispatch problems. Swarm Evol Comput 5:28–36. https://doi.org/10.1016/j.swevo.2012.03.001

Mehdinejad M, Mohammadi-Ivatloo B, Dadashzadeh-Bonab R, Zare K (2016) Solution of optimal reactive power dispatch of power systems using hybrid particle swarm optimization and imperialist competitive algorithms. Int J Electr Power Energy Syst 83:104–116. https://doi.org/10.1016/j.ijepes.2016.03.039

Mitchell M (1998) An introduction to genetic algorithms. MIT press, Cambridge

Moghadam A, Seifi AR (2014) Fuzzy-TLBO optimal reactive power control variables planning for energy loss minimization. Energy Convers Manage 77:208–215. https://doi.org/10.1016/j.enconman.2013.09.036

Mohseni-Bonab SM, Rabiee A, Mohammadi-Ivatloo B (2016a) Voltage stability constrained multi-objective optimal reactive power dispatch under load and wind power uncertainties: A stochastic approach. Renew Energy 85:598–609. https://doi.org/10.1016/j.renene.2015.07.021

Mohseni-Bonab SM, Rabiee A, Mohammadi-Ivatloo B, Jalilzadeh S, Nojavan S (2016b) A two-point estimate method for uncertainty modeling in multi-objective optimal reactive power dispatch problem. Int J Electr Power Energy Syst 75:194–204. https://doi.org/10.1016/j.ijepes.2015.08.009

Mouassa S, Bouktir T, Salhi A (2017) Ant lion optimizer for solving optimal reactive power dispatch problem in power systems. Eng Sci Technol, Int J 20(3):885–895. https://doi.org/10.1016/j.jestch.2017.03.006

Mukherjee A, Mukherjee V (2016) Chaos embedded krill herd algorithm for optimal VAR dispatch problem of power system. Int J Electr Power Energy Syst 82:37–48. https://doi.org/10.1016/j.ijepes.2016.02.039

Naderi E, Narimani H, Fathi M, Narimani MR (2017) A novel fuzzy adaptive configuration of particle swarm optimization to solve large-scale optimal reactive power dispatch. Appl Soft Comput 53:441–456. https://doi.org/10.1016/j.asoc.2017.01.012

Niknam T, Narimani MR, Azizipanah-Abarghooee R, Bahmani-Firouzi B (2013) Multiobjective optimal reactive power dispatch and voltage control: a new opposition-based self-adaptive modified gravitational search algorithm. IEEE Syst J 7(4):742–753. https://doi.org/10.1109/JSYST.2012.2227217

Nuaekaew K, Artrit P, Pholdee N, Bureerat S (2017) Optimal reactive power dispatch problem using a two-archive multi-objective grey wolf optimizer. Exp Syst Appl 87:79–89. https://doi.org/10.1016/j.eswa.2017.06.009

Polprasert J, Ongsakul W, Dieu VN (2016) Optimal Reactive power dispatch using improved pseudo-gradient search particle swarm optimization. Electr Power Compon Syst 44(5):518–532. https://doi.org/10.1080/15325008.2015.1112449

Radosavljević J, Jevtić M, Milovanović M (2016) A solution to the ORPD problem and critical analysis of the results. Electr Eng 100(1):253–265. https://doi.org/10.1007/s00202-016-0503-1

Raha SB, Chakraborty N, Biswas Raha S, Chakraborty N (2012) Tuned reactive power dispatch through modified differential evolution technique. Front Energy 6(2):138–147. https://doi.org/10.1007/s11708-012-0188-8

Rajan A, Malakar T (2015) Optimal reactive power dispatch using hybrid Nelder-Mead simplex based firefly algorithm. Int J Electr

Power Energy Syst 66:9–24. https://doi.org/10.1016/j.ijepes.2014.10.041
Rajan A, Malakar T (2016) Exchange market algorithm based optimum reactive power dispatch. Appl Soft Comput 43:320–336. https://doi.org/10.1016/j.asoc.2016.02.041
Ramesh S, Kannan S, Baskar S (2012) Application of modified NSGA-II algorithm to multi-objective reactive power planning. Appl Soft Comput 12(2):741–753. https://doi.org/10.1016/j.asoc.2011.09.015
Rao RVV, Savsani VJJ, Vakharia DPP (2011) Teaching-learning-based optimization: a novel method for constrained mechanical design optimization problems. Comput Aided Des 43(3):303–315. https://doi.org/10.1016/j.cad.2010.12.015
Rashedi E, Nezamabadi-pour H, Saryazdi S (2009) GSA: a gravitational search algorithm. Inf Sci 179(13):2232–2248. https://doi.org/10.1016/J.INS.2009.03.004
Rojas DG, Lezama JL, Villa W (2016) Metaheuristic techniques applied to the optimal reactive power dispatch: a review. IEEE Lat Am Trans 14(5):2253–2263. https://doi.org/10.1109/tla.2016.7530421
Roselyn JP, Devaraj D, Dash SS, Preetha Roselyn J, Devaraj D, Dash SS (2014) Multi objective differential evolution approach for voltage stability constrained reactive power planning problem. Int J Electr Power Energy Syst 59:155–165. https://doi.org/10.1016/j.ijepes.2014.02.013
Roy PK, Ghoshal SP, Thakur SS (2012a) Optimal VAR control for improvements in voltage profiles and for real power loss minimization using biogeography based optimization. Int J Electr Power Energy Syst 43(1):830–838. https://doi.org/10.1016/j.ijepes.2012.05.032
Roy PK, Mandal B, Bhattacharya K (2012b) Gravitational search algorithm based optimal reactive power dispatch for voltage stability enhancement. Electr Power Compon Syst 40(9):956–976. https://doi.org/10.1080/15325008.2012.675405
Sadollah A, Bahreininejad A, Eskandar H, Hamdi M (2013) Mine blast algorithm: a new population based algorithm for solving constrained engineering optimization problems. Appl Soft Comput 13(5):2592–2612
Saraswat A, Saini A (2013) Multi-objective optimal reactive power dispatch considering voltage stability in power systems using HFMOEA. Eng Appl Artif Intell 26(1):390–404. https://doi.org/10.1016/j.engappai.2012.06.008
Sehiemy RE, El-Ela AA, Shaheen A, Abou El-Ela A, El Sehiemy R, Sehiemy RE, El-Ela AA, Shaheen A (2013) Multi-objective fuzzy-based procedure for enhancing reactive power management. IET Gener Transm Distrib 7(12):1453–1460. https://doi.org/10.1049/iet-gtd.2013.0051
Seif Z, Ahmadi MB (2015) An opposition-based algorithm for function optimization. Eng Appl Artif Intell 37:293–306. https://doi.org/10.1016/j.engappai.2014.09.009
Shahbazi HR, Kalantar M (2013) The Optimal reactive power dispatch using seeker optimization algorithm based different objective functions. J Basic Appl Sci Res 3(8):232–240
Shaheen AM, El-Sehiemy RA, Farrag SM (2016) A novel adequate bi-level reactive power planning strategy. Int J Electr Power Energy Syst 78:897–909. https://doi.org/10.1016/j.ijepes.2015.12.004
Shaw B, Mukherjee V, Ghoshal SP (2014) Solution of reactive power dispatch of power systems by an opposition-based gravitational search algorithm. Int J Electr Power Energy Syst 55:29–40. https://doi.org/10.1016/j.ijepes.2013.08.010
Singh RP, Mukherjee V, Ghoshal SP (2015) Optimal reactive power dispatch by particle swarm optimization with an aging leader and challengers. Appl Soft Comput 29:298–309. https://doi.org/10.1016/j.asoc.2015.01.006
Soler EM, Asada EN, da Costa GRM (2013) Penalty-based nonlinear solver for optimal reactive power dispatch with discrete controls. IEEE Trans Power Syst 28(3):2174–2182. https://doi.org/10.1109/TPWRS.2013.2252207
Storn R, Price K (1997) Differential evolution—a simple and efficient heuristic for global optimization over continuous spaces. J Global Optim 11(4):341–359. https://doi.org/10.1023/a:1008202821328
Suganthan PN, Hansen N, Liang JJ, Deb K, Chen Y-P, Auger A, Tiwari S (2005) Problem definitions and evaluation criteria for the CEC 2005 special session on real-parameter optimization. KanGAL Rep 2005005:2005
Sulaiman MH, Mustaffa Z, Mohamed MR, Aliman O (2015) Using the gray wolf optimizer for solving optimal reactive power dispatch problem. Appl Soft Comput 32:286–292. https://doi.org/10.1016/j.asoc.2015.03.041
Tang X, Zhang H, Cui Y, Gu L, Deng Y (2013) A novel reactive power optimization solution using improved chaos PSO based on multi-agent architecture. Int Trans Electr Energy Syst 24(5):609–622. https://doi.org/10.1002/etep.1717
Thukaram D, Yesuratnam G (2008) Optimal reactive power dispatch in a large power system with AC-DC and FACTS controllers. IET Gener Transm Distrib 2(1):71. https://doi.org/10.1049/iet-gtd:20070163
Titare LS, Singh P, Arya LD, Choube SC (2014) Optimal reactive power rescheduling based on EPSDE algorithm to enhance static voltage stability. Int J Electr Power Energy Syst 63:588–599. https://doi.org/10.1016/j.ijepes.2014.05.078
Varadarajan M, Swarup KS (2008) Differential evolution approach for optimal reactive power dispatch. Appl Soft Comput 8(4):1549–1561. https://doi.org/10.1016/j.asoc.2007.12.002
Wang C, Liu Y, Zhao Y, Chen Y (2014) A hybrid topology scale-free Gaussian-dynamic particle swarm optimization algorithm applied to real power loss minimization. Eng Appl Artif Intell 32:63–75. https://doi.org/10.1016/j.engappai.2014.02.018
Xu Y, Zhang W, Liu W, Ferrese F (2012) Multiagent-based reinforcement learning for optimal reactive power dispatch. IEEE Trans Syst, Man, Cybern, Part C (appl Rev) 42(6):1742–1751. https://doi.org/10.1109/TSMCC.2012.2218596
Yalçın E, Çam E, Taplamacıoğlu MC (2019) A new chaos and global competitive ranking-based symbiotic organisms search algorithm for solving reactive power dispatch problem with discrete and continuous control variable. Electr Eng 102(2):573–590. https://doi.org/10.1007/S00202-019-00895-6
Yang X-S, Deb S (2009) Cuckoo search via Lévy flights. In: 2009 World Congress on Nature & Biologically Inspired Computing (NaBIC). IEEE. https://doi.org/10.1109/nabic.2009.5393690
Zhang X, Yu T, Yang B, Cheng L (2017) Accelerating bio-inspired optimizer with transfer reinforcement learning for reactive power optimization. Knowl-Based Syst 116:26–38. https://doi.org/10.1016/j.knosys.2016.10.024
Zhao B, Guo CX, Cao YJ (2005) A multiagent-based particle swarm optimization approach for optimal reactive power dispatch. IEEE Trans Power Syst 20(2):1070–1078. https://doi.org/10.1109/TPWRS.2005.846064
Zhihuan L, Yinhong L, Xianzhong D (2010) Non-dominated sorting genetic algorithm-II for robust multi-objective optimal reactive power dispatch. IET Gener Transm Distrib 4(9):1000. https://doi.org/10.1049/iet-gtd.2010.0105
Zhou B, Chan KW, Yu T, Wei H, Tang J (2014) Strength pareto multigroup search optimizer for multiobjective optimal reactive

power dispatch. IEEE Trans Industr Inf 10(2):1012–1022. https://doi.org/10.1109/TII.2014.2310634

Zimmerman RD, Murillo-Sanchez CE, Thomas RJ (2011) MATPOWER: steady-state operations, planning, and analysis tools for power systems research and education. IEEE Trans Power Syst 26(1):12–19. https://doi.org/10.1109/TPWRS.2010.2051168